European Journal of Control 80 (2024) 101127

Contents lists available at ScienceDirect

European Journal of Control

journal homepage: www.sciencedirect.com/journal/european-journal-of-control

Adaptive asymptotic tracking control of constrained nonlinear MIMO systems subject to unknown hysteresis input: A novel network-based strategy[☆]

Wei Zhao [a], Yu-Qun Han [a,b,c], Shan-Liang Zhu [a,b,c,*]

[a] School of Mathematics and Physics, Qingdao University of Science and Technology, Qingdao, China
[b] Qingdao Innovation Center of Artificial Intelligence Ocean Technology, Qingdao 266061, China
[c] The Research Institute for Mathematics and Interdisciplinary Sciences, Qingdao University of Science and Technology, Qingdao, China

ARTICLE INFO

Recommended by T Parisini

Keywords:
Multi-dimensional Taylor network
Asymptotic tracking control
Nonlinear MIMO systems
Unknown hysteresis
Time-varying full-state constraints

ABSTRACT

This paper presents a referential adaptive asymptotic tracking control scheme for nonlinear multi-input and multi-output (MIMO) systems with time-varying full-state constraints and unknown hysteresis input. In order to achieve good asymptotic tracking effect, a zero-limit positive continuous function is introduced into the adaptive backstepping design process while thoroughly considering the impact of disturbance-like terms on the tracking effect. Additionally, a new variable is also imported to replace the reciprocal of unknown coefficient of the Bouc–Wen hysteresis model. Then, a new adaptive law about the new variable is added by combining the positive function, which can not only lessen the impact of the unknown hysteresis input on the tracking effect, but also avoid the "singularity" problem. Aiming at the time-varying full-state constraints, a appropriate time-varying log-type barrier Lyapunov function (TLBLF) is constructed to ensure that all the states of the system are restricted within the constraint scope. Finally, a significant adaptive asymptotic tracking scheme is designed based on multi-dimensional Taylor network (MTN) approximation technology. Apart from achieving high-precision asymptotic tracking performance, the proposed scheme ensures the boundedness of all signals of the closed-loop system without violating the full-state constraints. And, three simulations are given to verify the effectiveness of the scheme.

1. Introduction

Tracking control of nonlinear systems has always been a significant research direction in control theory, which has been paid considerable attention to in the past decades. In order to achieve effective tracking control for nonlinear systems, various control methods have been proposed, such as adaptive backstepping control (Song et al., 2020; Xi et al., 2023; Zhao et al., 2019), H_∞ control (Liu et al., 2020; Zhao & Wang, 2022), sliding mode control (Echreshavi et al., 2022; Qi et al., 2023; Sun et al., 2023), fault-tolerant control (Zong et al., 2022). And it is universally acknowledged that adaptive backstepping control is a rather useful tool in dealing with control problems on nonlinear systems with parameter uncertainty. Consequently, it has been employed extensively in various nonlinear systems, such as switched systems (He et al., 2021; Wang & Long, 2022), stochastic systems (Chen et al., 2014; Meng et al., 2022; Sui et al., 2019), MIMO systems (Meng et al., 2015; Ruan et al., 2022). Nevertheless, not all system uncertainties can be linearly parameterized. Therefore, the traditional adaptive backstepping method cannot be used to construct the controller. In view of the above background, intelligent approximators, such as fuzzy logic systems (FLSs) and neural networks (NNs), attracted considerable attention which possess excellent ability to approximate unknown nonlinear terms. Since then, the combination of adaptive backstepping control and the above approximators has produced many fruitful results (Deng et al., 2022; Li & Li, 2021; Liang et al., 2022; Liu et al., 2023; Zhan et al., 2022; Zhu et al., 2023). It bears emphasizing that MTN, a special type of NNs, has been successfully integrated with adaptive backstepping control to effectively control nonlinear systems and has led to substantial notable research outcomes (Han, 2020; Han et al., 2021a; He et al., 2023; Li et al., 2022b). However, the aforementioned works just can achieve practical tracking control only when the tracking error is bounded without guaranteeing asymptotic convergence of the tracking error. In fact, high precision tracking effect is often required in practical system. Therefore, since asymptotic tracking control is

☆ This work was supported by the Shandong Provincial Natural Science Foundation, China (No. ZR2020QF055).
* Corresponding author at: School of Mathematics and Physics, Qingdao University of Science and Technology, Qingdao, China.
E-mail addresses: zhaowei_06@163.com (W. Zhao), yuqunhan@163.com (Y.-Q. Han), zhushanliang@qust.edu.cn (S.-L. Zhu).

https://doi.org/10.1016/j.ejcon.2024.101127
Received 30 March 2024; Received in revised form 1 September 2024; Accepted 12 October 2024
Available online 19 October 2024
0947-3580/© 2024 European Control Association. Published by Elsevier Ltd. All rights are reserved, including those for text and data mining, AI training, and similar technologies.

more suitable for the actual industrial process, it has aroused much attention among scholars, which can be seen in Li et al. (2022a), Ma et al. (2022), Pan et al. (2022). For example, authors in Ma et al. (2022) realized asymptotic tracking control for nonlinear systems with actuator faults by introducing a novel σ-modification term. Authors in Pan et al. (2022) studied the asymptotic tracking control problem for MIMO systems with unknown control directions. However, all the above works ignore the influence of hysteresis on tracking performance.

Actually, with the constant enhance of system performance requirements in modern industry, many new physical materials such as magnetostriction are gradually applied. So, hysteresis effect is challenging to eliminate in real-world systems such as biology optics, mechanical actuators, and electronic relay circuits. Furthermore, it is important to recognize that hysteresis, being a nonlinear characteristic, can undermine the stability of the controlled system. Therefore, how to reduce the influence of hysteresis on the system stability and improve the control effect has been one of the pretty essential research hotspots. Up to now, many excellent research schemes have been produced to solve the above problem (Han et al., 2022; Liu et al., 2021; Su et al., 2021; Wang et al., 2022b; Wu et al., 2023; Xu et al., 2022; Zhang et al., 2022). For example, authors in Han et al. (2022) combined the Nussbaum-type function with adaptive backstepping method to deal with the influence of Bouc–Wen hysteresis on the system stability. Moreover, the authors of Capuano et al. (2022) proposed a more accurate and computationally efficient solution algorithm for a modified Bouc–Wen hysteresis. Authors in Zhang et al. (2022) used the PI model to describe the asymmetric hysteresis, and compensated the hysteresis effect by constructing an implicit inverse compensator. Authors in Liu et al. (2021) counteract the state hysteresis by incorporating the inverse hysteresis model into the adaptive backstepping method. Additionally, authors in Vaiana and Rosati (2023a, 2023b) studied the rate-independent hysteresis model. However, all the control schemes proposed in the above work are no longer applicable to constrained systems. To put it simply, the control effect achieved by the above schemes is greatly reduced for constrained systems.

As is known to all, constraints problem such as state constraint (Gao et al., 2022; Xie et al., 2022b) are inevitable in some practical physical systems. In fact, states in real systems are almost always limited. Therefore, once the full-state constraints issue is ignored, the instability of the controlled system will be caused. Recently, a lot of work has been done on full-state constraints (Gao et al., 2022; Jin & Li, 2021; Wang et al., 2022a; Xie et al., 2022a, 2022b). Authors in Wang et al. (2022a) used one-to-one nonlinear mapping to handle full-state constraints. Different from Wang et al. (2022a), authors in Li et al. (2022b) proposed a novel asymmetric time-varying BLFs to cope with full-state constraints. On this basis, (Xie et al., 2022a) further implemented asymptotic tracking control by introducing a positive integrable function to design the controller for the state-constrained system, ensuring that the tracking error tends to zero asymptotically.

However, it is important to note that in many practical engineering systems, it is quite common for full-state constraints and hysteresis phenomenon to exist simultaneously. For example, in electric motor control, hysteresis phenomenon often occurs in permanent magnet synchronous motors, induction motors, and other types of motors. For applications requiring high-precision control, it is crucial to consider the influence of hysteresis on the system's dynamic characteristics. And full-state constraints can be adopted to design controllers that ensure the system operates within performance requirements and state boundaries. Therefore, how to solve the coexistence problem in the framework of asymptotic tracking control is a very potential research direction. Motivated by this, this paper displays a MTN-based adaptive asymptotic tracking control scheme for nonlinear MIMO systems with Bouc–Wen input hysteresis and time-varying full-state constraints. Firstly, in order to solve the time-varying full-state constraints problem, a novel TLBLF is introduced. Additionally, the Bouc–Wen hysteresis model is applied to describe the hysteresis nonlinearity, and an adaptive law is designed ingeniously by approximating the inverse of the completely unknown coefficient of the hysteresis model. More importantly, in order to realize a satisfactory tracking effect, intermediate adaptive laws about disturbance-like items are added. Meanwhile, positive continuous functions are introduced which are designed into the controllers and adaptive laws to obtain the high-precision asymptotic tracking control effect. In contrast to prior work, this paper presents several key contributions as follows:

(1) For nonlinear MIMO systems with time-varying full-state constraints and unknown hysteresis input, an innovative adaptive asymptotic tracking control scheme based on MTN technology has been put forward. MTN is leveraged to approximate the unknown nonlinear terms, consequently reducing the computational burden and simplifying the controller structure. Although the MTN approximation technique is widely applied in nonlinear systems (Du et al., 2023; Han et al., 2021b; Zhu & Han, 2022), its application has not been extended to MIMO nonlinear systems that are subjected to both time-varying full-state constraints and input hysteresis.
(2) Unlike the approaches in Refs. Liu et al. (2021), Qiu et al. (2020), this paper opts not to compensate for hysteresis through the construction of an inverse hysteresis model or direct approximation of the unknown slope parameters of the hysteresis model. Instead, by approximating the reciprocal of the entirely unknown parameters of the hysteresis model, an additional adaptive law is incorporated to mitigate the impact of hysteresis nonlinearity on system stability. This method not only simplifies the controller design process but also effectively circumvents the "singularity" issue.
(3) What makes this paper different from Jin and Li (2021), Li et al. (2022b), Su et al. (2021) lies in that it not only takes time-varying full-state constraints and input hysteresis into consideration simultaneously, but also extends the actual tracking control to asymptotic tracking control by introducing a zero-limit positive continuous function into the controllers and adaptive laws. Most importantly, in order to achieve the high-precision asymptotic tracking control effect, intermediate adaptive laws about disturbance-like items are also fully considered.

2. Problem statement and preliminary knowledge

2.1. Problem statement

This paper considers the following nonlinear MIMO systems with unknown hysteresis input:

$$\begin{cases} \dot{\chi}_{m,j} = \chi_{m,j+1} + \Gamma_{m,j}\left(\bar{\chi}_{m,j}\right) + \phi_{m,j}\left(\bar{\chi}_{m,j}\right) \\ \quad j = 1, \dots, n_m - 1 \\ \dot{\chi}_{m,n_m} = u_m + \Gamma_{m,n_m}(\chi) + \phi_{m,n_m}\left(\bar{\chi}_{m,n_m}\right) \\ \quad y_m = \chi_{m,1} \end{cases} \tag{1}$$

where $m = 1, \dots, n$. $\bar{\chi}_{m,j} = [\chi_{m,1}, \chi_{m,2}, \dots, \chi_{m,j}]^{\mathrm{T}} \in R^j$ represents the state vector of the system with $\chi = [\bar{\chi}_{1,n_1}, \dots, \bar{\chi}_{m,n_m}]^{\mathrm{T}}$. $\Gamma_{m,j}(\cdot)$ denotes unknown nonlinear smooth function with $\Gamma_{m,j}(0) = 0$. $\phi_{m,j}$ is defined as the unknown but bounded time-varying disturbance. $y_m \in R$ represents the output of the controlled system. u_m is the control input and the output of the hysteresis. For the purpose of addressing the issue of hysteresis input on system stability, the following Bouc–Wen hysteresis model is introduced to characterize the hysteresis nonlinearity:

$$u_m = \pounds_m(v_m) = \ell_{m,1} v_m + \ell_{m,2} \varrho_m \tag{2}$$

where v_m is the hysteresis input. $\ell_{m,1}$, $\ell_{m,2}$ are unknown parameters with $\mathrm{sgn}(\ell_{m,1}) = \mathrm{sgn}(\ell_{m,2})$. $\mathrm{sgn}(*)$ is the sign function of $*$. ϱ_m is the

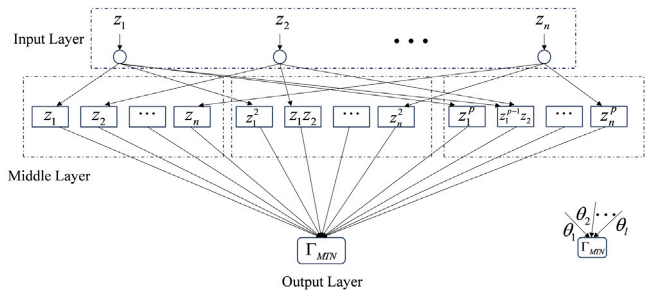

Fig. 1. The structural diagram of MTN.

auxiliary variable, satisfying the following differential equation:

$$\dot{\varrho}_m = \dot{v}_m - \iota\left|\dot{v}_m\right|\left|\varrho_m\right|^{\kappa-1}\varrho_m - \bar{\varphi}\dot{v}_m\left|\varrho_m\right|^{\kappa} \equiv \dot{v}_m\Delta(\varrho_m, \dot{v}_m) = 0 \tag{3}$$

where ι, $\bar{\varphi}$ and κ are hysteresis parameters with $\iota > |\bar{\varphi}|$, $\kappa > 1$. Moreover, based on (3), $\Delta(\varrho_m, \dot{v}_m)$ is

$$\Delta(\varrho_m, \dot{v}_m) = 1 - \text{sgn}(\dot{v}_m)\iota\left|\varrho_m\right|^{\kappa-1}\varrho_m - \bar{\varphi}\left|\varrho_m\right|^{\kappa} \tag{4}$$

According to Han et al. (2022), Wang et al. (2016), ϱ_m is bounded and satisfies

$$\left|\varrho_m\right| \le \varrho_m^* = \sqrt[\kappa]{\frac{1}{\iota + \bar{\varphi}}} \tag{5}$$

where $\varrho_m^* > 0$ is the constant.

Remark 1. The states of the closed-loop system (1) are confined in a compact set: $\Omega_\chi := \left\{\chi_{m,j} \in R, \left|\chi_{m,j}\right| \le \emptyset_{c_{m,j}}(t)\right\}$ with $\emptyset_{c_{m,j}}(t) : R^+ \to R^+$, for $, m = 1, 2, \ldots, n$.

The primary goals of this paper are to design the adaptive asymptotic tracking controller to make sure that

(i) the system output y_m could asymptotically track the reference signal $y_{m,r}$;

(ii) all signals of the closed-loop system are bounded;

(iii) all states $\chi_{m,j}$ are within the given constraint range, namely, $\left|\chi_{m,j}\right| \le \emptyset_{c_{m,j}}(t)$ with $\emptyset_{c_{m,j}}(t) : R^+ \to R^+$, for $m = 1, 2, \ldots, n$, $j = 1, \ldots, n_m$.

2.2. Multi-dimensional Taylor network

In this paper, MTNs will be used to approximate unknown nonlinear functions. It is worth emphasizing that MTN is a new kind of feedforward neural networks, the structural diagram of MTN is shown as Fig. 1, where $z_1, z_2, \ldots, z_n$ are the input of MTN and $\theta = \left[\theta_1, \theta_2, \ldots, \theta_l\right]^{\mathrm{T}} \in R^l$ is the weight vector of MTN. For more details on the MTN, see Du et al. (2023), Han et al. (2022), Zhu and Han (2022), here, only the following Lemma is given.

Lemma 1 (*Du et al. (2023), Han et al. (2022), Zhao et al. (2024a, 2024), Zhu and Han (2022)*). *Supposing $\Gamma(z)$ is a continuous and unknown function defined on the compact set $\Omega_z \in R^n$, for constant $\bar{\Psi} > 0$, there exists a MTN used to estimate $\Gamma(z)$ such that*

$$\Gamma(z) = \theta^{\mathrm{T}} H_{p_n}(z) + \Psi(z) \tag{6}$$

where $z = \left[z_1, z_2, \ldots, z_n\right]^{\mathrm{T}} \in R^n$ and $\theta = \left[\theta_1, \theta_2, \ldots, \theta_l\right]^{\mathrm{T}} \in R^l$ are the input vector and the weight vector of MTN, respectively. $\Psi(z)$ denotes the error generated in the estimation with $|\Psi(z)| \le \bar{\Psi}$. $H_{p_n}(z)$ represents the middle intermediate input layer of MTN, which can be described as $H_{p_n}(z) = [z_1, \ldots, z_n, z_1^2, z_1 z_2, \ldots, z_1 z_n, z_2 z_3, \ldots, z_n^2, \ldots, z_1^p, \ldots, z_n^p]^{\mathrm{T}}$.

Remark 2. MTN is a network structure similar to the radial basis function neural network (RBFNN) in existing research (Deng et al., 2022; Li & Li, 2021; Zhu et al., 2023), consisting of three layers: input layer, middle layer, and output layer. Unlike the middle layer of RBFNN, MTN is composed of a set of polynomials instead of a Gaussian function set, effectively simplifying the structure of RBFNN and reducing computational complexity.

2.3. Preliminary knowledge

In order to facilitate the design of the control scheme, some necessary Assumptions as well as Lemmas are presented as follows.

Assumption 1. $\phi_{m,j}(\cdot)$ is a bounded and unknown time-varying function. Then, there exists a constant $\bar{\phi}_{m,j} > 0$, such that

$$\left|\phi_{m,j}(\cdot)\right| \le \bar{\phi}_{m,j} \tag{7}$$

Assumption 2. The reference signal $y_{m,r}$ and its kth time derivative $y_{m,r}^{(k)}$ are continuous and bounded. Meanwhile, there exist several functions $\Lambda_{m,j}(t) : R^+ \to R^+$, $m = 1, \ldots, n, j = 0, \ldots, n_m - 1$ satisfy $\left|y_{m,r}\right| \le \Lambda_{m,0}(t)$ and $\left|y_{m,r}^{(k)}\right| \le \Lambda_{m,j}(t)$, $k = 0, 1, \ldots, n_m$, $\forall t \ge 0$, where $\bar{\Lambda}_{m,0}$ is the upper bound of $\Lambda_{m,0}$.

Remark 3. Assumption 1 shows that the disturbance of the system (1) is bounded, which will be used in the subsequent design of the controller. This assumption is a normal assumption for nonlinear systems with external disturbance, as can be seen in Han (2020).

Remark 4. Assumption 2 implies that the reference signal $y_{m,r}$ can be used for controller design, which is a common consideration in tracking control problem for nonlinear system. The limits on the reference signal $y_{m,r}$ and its derivatives $y_{m,r}^{(k)}$ are widely adopted in full-state constraint condition, as cited in Refs. Lan et al. (2021), Li et al. (2022b). This assumption makes it feasible to design a controller that satisfies full-state constraints.

Lemma 2 (*Sun et al. (2019), Xie et al. (2022a),Barbalat Lemma*). *For continuous and unknown function $\Pi(t) : R^+ \to R^+$, if $\lim_{t\to\infty}\Pi(t) = 0$, then $\int_0^\infty \Pi(\epsilon)d\epsilon = \bar{\Pi} < \infty$ holds, where $\bar{\Pi}$ is a known nonnegative constant.*

Lemma 3 (*Sun et al. (2019)*). *$\tilde{\omega}(t)$ is a uniformly continuous function defined on $[0, \infty)$. Suppose $\int_0^\infty \tilde{\omega}(\epsilon)d\epsilon$ exists and is finite. Then, $\lim_{t\to\infty}\tilde{\omega}(t) = 0$ holds.*

Lemma 4 (*Han et al. (2021a), He et al. (2023),Young's Inequality*). *For $\forall(\Phi_m, \Lambda_m) \in R^2$, the following inequality holds*

$$\Phi_m\Lambda_m \le \frac{\varepsilon_m^\mu}{\mu}\left|\Phi_m\right|^\mu + \frac{1}{\nu\varepsilon_m^\nu}\left|\Lambda_m\right|^\nu \tag{8}$$

where $\varepsilon_m > 0$ is the constant. $\mu > 1$ and $\nu > 1$ with $(\mu - 1)(\nu - 1) = 1$.

Lemma 5 (*Li et al. (2022b)*). *For $\forall\Theta \in R$ and $\forall Y_c \in R^+$, if $|\Theta| < Y_c$, the following inequality holds*

$$\ln\frac{Y_c^{2s}}{Y_c^{2s} - \Theta^{2s}} < \frac{\Theta^{2s}}{Y_c^{2s} - \Theta^{2s}} \tag{9}$$

where $s > 0$ is a constant, and $\ln(\cdot)$ is the logarithmic of $\cdot$.

3. Main results

3.1. Controller design

In this section, an adaptive asymptotic tracking controller for MIMO systems (1) is designed. The controller design is based on the following coordinate transformation.

$$\begin{cases} z_{m,1} = \chi_{m,1} - y_{m,r} \\ z_{m,j} = \chi_{m,j} - \alpha_{m,j-1} \end{cases} \tag{10}$$

where $m = 1, \dots, n, j = 1, \dots, n_m$. $y_{m,r}$ is the reference signal. $\alpha_{m,j-1}$ is the virtual control signal satisfying $\alpha_{m,j-1} \le \Lambda_{m,j-1}(t)$.

In order to handle time-varying full-state constraints, referring to (Jin & Li, 2021; Li et al., 2022b), construct TLBLFs $V^{\iota}_{m,j}$ as:

$$V^{\iota}_{m,j} = \frac{1}{2}\ln\left(\frac{\emptyset^2_{b_{m,j}}(t)}{\emptyset^2_{b_{m,j}}(t) - z^2_{m,j}}\right) \tag{11}$$

where $z_{m,j} \in \Omega_z := \{z_{m,j} \in R, \left|z_{m,j}\right| < \emptyset_{b_{m,j}}(t)\}$ with $\emptyset_{b_{m,1}}(t) = \emptyset_{c_{m,1}}(t) - \Lambda_{m,0}(t)$, $\emptyset_{b_{m,j}}(t) = \emptyset_{c_{m,j}}(t) - \Lambda_{m,j-1}(t)$, $m = 1, \dots, n, j = 2, \dots, n_m$.

Remark 5. Compared with the existing BLFs such as tan-type BLFs and integral BLFs, (11) may simplify controller design because of its simpler mathematical form, leading to improved computational efficiency in control tasks. Meanwhile, it can handle both constant and time-varying constraints, making it more widely applicable in constraint control. And for simplicity of calculation, the variable t will be ignored in the following.

Then, taking the time derivative of (11), one has

$$\dot{V}^{\iota}_{m,j} = \frac{\dot{\emptyset}_{b_{m,j}}}{\emptyset_{b_{m,j}}} - \frac{\emptyset_{b_{m,j}}\dot{\emptyset}_{b_{m,j}} - z_{m,j}\dot{z}_{m,j}}{\emptyset^2_{b_{m,j}} - z^2_{m,j}} \tag{12}$$

The detailed process of controller design is given below.

Step $m, 1 (1 \le m \le n)$: The existence of hysteresis nonlinearity and unknown functions brings great obstacles to achieve asymptotic tracking control. Therefore, the following Lyapunov function $V_{m,1}$ is considered

$$V_{m,1} = V^{\iota}_{m,1} + \frac{1}{2}\tilde{\lambda}^2_{m,1} + \frac{1}{2}\tilde{\Xi}^2_{m,1} \tag{13}$$

where $\lambda_{m,1} = \|\theta_{m,1}\|$ denotes unknown constant, $\theta_{m,1}$ is the weight vector of MTN. $\tilde{\lambda}_{m,1} = \lambda_{m,1} - \hat{\lambda}_{m,1}$ and $\hat{\lambda}_{m,1}$ is the estimation of $\lambda_{m,1}$. $\tilde{\lambda}_{m,1}$ is the estimation error. Similarly, $\tilde{\Xi}_{m,1} = \Xi_{m,1} - \hat{\Xi}_{m,1}$ is the estimation error with $\Xi_{m,1} = \bar{\Psi}_{m,1} + \bar{\phi}_{m,1}$.

Remark 6. In this paper, $\Xi_{m,j}$ is defined to compensate for the disturbance-like items including approximation error $\Psi_{m,j}$ generated by the process of MTN approximating unknown nonlinear term, the bounded disturbance $\phi_{m,j}$ and the bounded term ϱ_m of the input hysteresis model. Furthermore, in order to reduce the influence of the above disturbance-like items on the tracking effect, the positive continuous functions $\Pi_{m,j}(t)$ are introduced into adaptive laws and controllers to realize the asymptotic tracking control.

Denote $\pounds_{b_{m,1}} = \frac{z_{m,1}}{\emptyset_{b_{m,1}}}$ and $\vartheta_{m,1} = \frac{1}{\emptyset^2_{b_{m,1}} - z^2_{m,1}}$, then, the time derivative of $V_{m,1}$ is transformed into the following form by combining (13)

$$\begin{aligned}\dot{V}_{m,1} &= \dot{V}^{\iota}_{m,1} - \tilde{\lambda}_{m,1}\dot{\hat{\lambda}}_{m,1} - \tilde{\Xi}_{m,1}\dot{\hat{\Xi}}_{m,1} \\ &= \vartheta_{m,1}z_{m,1}\dot{z}_{m,1} - \tilde{\lambda}_{m,1}\dot{\hat{\lambda}}_{m,1} \\ &- \left[\frac{\dot{\emptyset}_{b_{m,1}}}{\emptyset_{b_{m,1}}}\frac{\pounds_{b_{m,1}}}{\emptyset_{b_{m,1}}(1-\pounds^2_{b_{m,1}})}\right]z_{m,1} - \tilde{\Xi}_{m,1}\dot{\hat{\Xi}}_{m,1}\end{aligned} \tag{14}$$

Then, based on (1) and (10), the time derivative of $z_{m,1}$ is

$$\dot{z}_{m,1} = \dot{\chi}_{m,1} - \dot{y}_{m,r} = \chi_{m,2} + \Gamma_{m,1} + \phi_{m,1} - \dot{y}_{m,r} \tag{15}$$

Furthermore, by combining (14) and (15), the time derivative of $V_{m,1}$ becomes

$$\begin{aligned}\dot{V}_{m,1} &= \vartheta_{m,1}z_{m,1}\left(\chi_{m,2} + \tilde{\Gamma}_{m,1}\right) - \vartheta^2_{m,1}z^2_{m,1} \\ &+ \vartheta_{m,1}z_{m,1}\phi_{m,1} - \tilde{\lambda}_{m,1}\dot{\hat{\lambda}}_{m,1} - \tilde{\Xi}_{m,1}\dot{\hat{\Xi}}_{m,1}\end{aligned} \tag{16}$$

where $\tilde{\Gamma}_{m,1} = \Gamma_{m,1} - \dot{y}_{m,r} - \frac{1}{\vartheta_{m,1}}\frac{\dot{\emptyset}_{b_{m,1}}}{\emptyset_{b_{m,1}}}\frac{\pounds_{b_{m,1}}}{\emptyset_{b_{m,1}}(1-\pounds^2_{b_{m,1}})} + \vartheta_{m,1}z_{m,1}$ is a combination of nonlinear functions. Based on the MTN approximation technique in Lemma 1, for any constant $\bar{\Psi}_{m,1} > 0$, $\tilde{\Gamma}_{m,1}$ can be approximated by one MTN, that is, the following formula can be established

$$\tilde{\Gamma}_{m,1} = \theta^{\mathrm{T}}_{m,1}H_{p_{m,1}} + \Psi_{m,1}, |\Psi_{m,1}| \le \bar{\Psi}_{m,1} \tag{17}$$

where $\Psi_{m,1}$ is the approximation error of the combination term $\tilde{\Gamma}_{m,1}$ and $\theta^{\mathrm{T}}_{m,1}H_{p_{m,1}}$.

Then, substituting (17) into (16) and taking (10) into account, it can be obtained that

$$\begin{aligned}\dot{V}_{m,1} &= \vartheta_{m,1}z_{m,1}\left(z_{m,2} + \alpha_{m,1}\right) - \vartheta^2_{m,1}z^2_{m,1} \\ &+ \vartheta_{m,1}z_{m,1}\theta^{\mathrm{T}}_{m,1}H_{p_{m,1}} + \vartheta_{m,1}z_{m,1}(\phi_{m,1} + \Psi_{m,1}) \\ &- \tilde{\lambda}_{m,1}\dot{\hat{\lambda}}_{m,1} - \tilde{\Xi}_{m,1}\dot{\hat{\Xi}}_{m,1}\end{aligned} \tag{18}$$

Moreover, if $\forall\zeta \in R$, $\wp > 0$ holds, then, $0 \le |\zeta| - \frac{\zeta^2}{\sqrt{\zeta^2+\wp^2}} < \wp$ will hold. So, combining it with (18), the following inequality holds

$$\begin{aligned}&\vartheta_{m,1}z_{m,1}\theta^{\mathrm{T}}_{m,1}H_{p_{m,1}} + \vartheta_{m,1}z_{m,1}(\phi_{m,1} + \Psi_{m,1}) \\ &\le \frac{\lambda_{m,1}\vartheta^2_{m,1}z^2_{m,1}H^{\mathrm{T}}_{p_{m,1}}H_{p_{m,1}}}{\sqrt{\vartheta^2_{m,1}z^2_{m,1}H^{\mathrm{T}}_{p_{m,1}}H_{p_{m,1}} + \Pi^2_{m,1}}} + \lambda_{m,1}\Pi_{m,1} \\ &+ \frac{\Xi_{m,1}\vartheta^2_{m,1}z^2_{m,1}}{\sqrt{\vartheta^2_{m,1}z^2_{m,1} + \Pi^2_{m,1}}} + \Xi_{m,1}\Pi_{m,1}\end{aligned} \tag{19}$$

Applying Lemma 4 on $\vartheta_{m,1}z_{m,1}z_{m,2}$ gives

$$\vartheta_{m,1}z_{m,1}z_{m,2} \le \frac{1}{2}\vartheta^2_{m,1}z^2_{m,1} + \frac{1}{2}z^2_{m,2} \tag{20}$$

Then, substituting (19) and (20) into (18), $\dot{V}_{m,1}$ can be changed into

$$\begin{aligned}\dot{V}_{m,1} &\le \vartheta_{m,1}z_{m,1}\alpha_{m,1} + \vartheta_{m,1}z_{m,1}\frac{\hat{\Xi}_{m,1}\vartheta_{m,1}z_{m,1}}{\sqrt{\vartheta^2_{m,1}z^2_{m,1}\Pi^2_{m,1}}} \\ &+ \vartheta_{m,1}z_{m,1}\frac{\hat{\lambda}_{m,1}\vartheta_{m,1}z_{m,1}H^{\mathrm{T}}_{p_{m,1}}H_{p_{m,1}}}{\sqrt{\vartheta^2_{m,1}z^2_{m,1}H^{\mathrm{T}}_{p_{m,1}}H_{p_{m,1}} + \Pi^2_{m,1}}} \\ &+ \tilde{\lambda}_{m,1}(\tau_{m,1} - \dot{\hat{\lambda}}_{m,1}) + \tilde{\Xi}_{m,1}(\iota_{m,1} - \dot{\hat{\Xi}}_{m,1}) \\ &+ \frac{1}{2}z^2_{m,2} + \Pi_{m,1}(\lambda_{m,1} + \Xi_{m,1})\end{aligned} \tag{21}$$

where $\tau_{m,1} = \frac{\vartheta^2_{m,1}z^2_{m,1}H^{\mathrm{T}}_{p_{m,1}}H_{p_{m,1}}}{\sqrt{\vartheta^2_{m,1}z^2_{m,1}H^{\mathrm{T}}_{p_{m,1}}H_{p_{m,1}}+\Pi^2_{m,1}}}$, $\iota_{m,1} = \frac{\vartheta^2_{m,1}z^2_{m,1}}{\sqrt{\vartheta^2_{m,1}z^2_{m,1}+\Pi^2_{m,1}}}$.

According to the adaptive backstepping design process, the following virtual controller and adaptive laws are given

$$\begin{aligned}\alpha_{m,1} &= -\mu_{m,1}z_{m,1} - \frac{\vartheta_{m,1}z_{m,1}\hat{\Xi}_{m,1}}{\sqrt{\vartheta^2_{m,1}z^2_{m,1} + \Pi^2_{m,1}}} \\ &- \frac{\vartheta_{m,1}z_{m,1}\hat{\lambda}_{m,1}H^{\mathrm{T}}_{p_{m,1}}H_{p_{m,1}}}{\sqrt{\vartheta^2_{m,1}z^2_{m,1}H^{\mathrm{T}}_{p_{m,1}}H_{p_{m,1}} + \Pi^2_{m,1}}}\end{aligned} \tag{22}$$

$$\dot{\hat{\lambda}}_{m,1} = \tau_{m,1} - \Pi_{m,1}\hat{\lambda}_{m,1} \tag{23}$$

$$\dot{\hat{\Xi}}_{m,1} = \iota_{m,1} - \Pi_{m,1}\hat{\Xi}_{m,1} \tag{24}$$

where $\mu_{m,1} > 0$ is the design parameter.

Then, integrating (21)–(24), the time derivative of $V_{m,1}$ can be transformed as

$$\begin{aligned}\dot{V}_{m,1} &\le -\mu_{m,1}\vartheta_{m,1}z^2_{m,1} + \frac{1}{2}z^2_{m,2} + \Pi_{m,1}(\lambda_{m,1} + \Xi_{m,1}) \\ &+ \Pi_{m,1}\tilde{\lambda}_{m,1}\hat{\lambda}_{m,1} + \Pi_{m,1}\tilde{\Xi}_{m,1}\hat{\Xi}_{m,1}\end{aligned} \tag{25}$$

Remark 7. $\frac{1}{2}z^2_{m,2}$ will be coped with in step $m, 2$.

Step $m, k (1 \le m \le n, 2 \le k \le n_m - 1)$: Similar to (13), the following Lyapunov function $V_{m,k}$ is considered

$$V_{m,k} = V_{m,k-1} + V^{\iota}_{m,k} + \frac{1}{2}\tilde{\lambda}^2_{m,k} + \frac{1}{2}\tilde{\Xi}^2_{m,k} \tag{26}$$

where $\lambda_{m,k} = \|\theta_{m,k}\|$ denotes unknown constant, $\theta_{m,k}$ is the weight vector of MTN. $\tilde{\lambda}_{m,k} = \lambda_{m,k} - \hat{\lambda}_{m,k}$ and $\hat{\lambda}_{m,k}$ is the estimation of $\lambda_{m,k}$. $\tilde{\lambda}_{m,k}$ is the estimation error. Similarly, $\tilde{\Xi}_{m,k} = \Xi_{m,k} - \hat{\Xi}_{m,k}$ is the estimation error with $\Xi_{m,k} = \bar{\Psi}_{m,k} + \bar{\phi}_{m,k}$.

Denote $\pounds_{\varnothing_{m,k}} = \frac{z_{m,k}}{\varnothing_{b_{m,k}}}$ and $\vartheta_{m,k} = \frac{1}{\varnothing^2_{b_{m,k}} - z^2_{m,k}}$. Then, taking the time derivative of $V_{m,k}$, one has

$$\begin{aligned}\dot{V}_{m,k} &= \dot{V}^{\iota}_{m,k} - \tilde{\lambda}_{m,k}\dot{\hat{\lambda}}_{m,k} - \tilde{\Xi}_{m,k}\dot{\hat{\Xi}}_{m,k} + \dot{V}_{m,k-1} \\ &= \vartheta_{m,k} z_{m,k} \dot{z}_{m,k} - \tilde{\lambda}_{m,k}\dot{\hat{\lambda}}_{m,k} - \tilde{\Xi}_{m,k}\dot{\hat{\Xi}}_{m,k} \\ &\quad - \left[\frac{\dot{\varnothing}_{b_{m,k}}}{\varnothing_{b_{m,k}}} \frac{\pounds_{b_{m,k}}}{\varnothing_{b_{m,k}}(1-\pounds^2_{b_{m,k}})}\right] z_{m,k} + \dot{V}_{m,k-1}\end{aligned} \tag{27}$$

Then, based on (1) and (10), the time derivative of $z_{m,k}$ is

$$\dot{z}_{m,k} = \chi_{m,k+1} + \Gamma_{m,k} + \phi_{m,k} - \dot{\alpha}_{m,k-1} \tag{28}$$

Furthermore, combining (27) and (28), the time derivative of $V_{m,k}$ becomes

$$\begin{aligned}\dot{V}_{m,k} &= \vartheta_{m,k} z_{m,k}(\chi_{m,k+1} + \tilde{\Gamma}_{m,k}) - \frac{1}{2}z^2_{m,k} \\ &\quad - \vartheta^2_{m,k} z^2_{m,k} + \vartheta_{m,k} z_{m,k}\phi_{m,k} - \tilde{\lambda}_{m,k}\dot{\hat{\lambda}}_{m,k} \\ &\quad - \tilde{\Xi}_{m,k}\dot{\hat{\Xi}}_{m,k} + \dot{V}_{m,k-1}\end{aligned} \tag{29}$$

where $\tilde{\Gamma}_{m,k} = \Gamma_{m,k} - \dot{\alpha}_{m,k-1} - \frac{1}{\vartheta_{m,k}} \frac{\dot{\varnothing}_{b_{m,k}}}{\varnothing_{b_{m,k}}} \frac{\pounds_{b_{m,k}}}{\varnothing_{b_{m,k}}(1-\pounds^2_{b_{m,k}})} + \vartheta_{m,k} z_{m,k} + \frac{1}{2\vartheta_{m,k}} z_{m,k}$ is a combination of nonlinear functions. Based on the MTN approximation technique in Lemma 1, for any constant $\bar{\Psi}_{m,k} > 0$, $\tilde{\Gamma}_{m,k}$ can be approximated by one MTN, that is, the following formula can be established

$$\tilde{\Gamma}_{m,k} = \theta^{\mathrm{T}}_{m,k} H_{p_{m,k}} + \Psi_{m,k}, |\Psi_{m,k}| \le \bar{\Psi}_{m,k} \tag{30}$$

where $\Psi_{m,k}$ is the approximation error of the combination term $\tilde{\Gamma}_{m,k}$ and $\theta^{\mathrm{T}}_{m,k} H_{p_{m,k}}$.

Then, substituting (30) into (29) and taking (10) into account, it can be obtained that

$$\begin{aligned}\dot{V}_{m,k} &= \vartheta_{m,k} z_{m,k}\left(z_{m,k+1} + \alpha_{m,k}\right) - \vartheta^2_{m,k} z^2_{m,k} \\ &\quad + \vartheta_{m,k} z_{m,k}\theta^{\mathrm{T}}_{m,k} H_{p_{m,k}} + \vartheta_{m,k} z_{m,k}(\phi_{m,k} + \Psi_{m,k}) \\ &\quad - \frac{1}{2}z^2_{m,k} - \tilde{\lambda}_{m,k}\dot{\hat{\lambda}}_{m,k} - \tilde{\Xi}_{m,k}\dot{\hat{\Xi}}_{m,k} + \dot{V}_{m,k-1}\end{aligned} \tag{31}$$

Similar to (19) in step $m,1$, one has

$$\begin{aligned}&\vartheta_{m,k} z_{m,k}\theta^{\mathrm{T}}_{m,k} H_{p_{m,k}} + \vartheta_{m,k} z_{m,k}(\phi_{m,k} + \Psi_{m,k}) \\ &\le \frac{\lambda_{m,k}\vartheta^2_{m,k} z^2_{m,k} H^{\mathrm{T}}_{p_{m,k}} H_{p_{m,k}}}{\sqrt{\vartheta^2_{m,k} z^2_{m,k} H^{\mathrm{T}}_{p_{m,k}} H_{p_{m,k}} + \Pi^2_{m,k}}} + \lambda_{m,k}\Pi_{m,k} \\ &\quad + \frac{\Xi_{m,k}\vartheta^2_{m,k} z^2_{m,k}}{\sqrt{\vartheta^2_{m,k} z^2_{m,k} + \Pi^2_{m,k}}} + \Xi_{m,k}\Pi_{m,k}\end{aligned} \tag{32}$$

Applying Lemma 4 on $\vartheta_{m,k} z_{m,k} z_{m,k+1}$ gives

$$\vartheta_{m,k} z_{m,k} z_{m,k+1} \le \frac{1}{2}\vartheta^2_{m,k} z^2_{m,k} + \frac{1}{2}z^2_{m,k+1} \tag{33}$$

Then, substituting (32) and (33) into (31), the time derivative of $V_{m,k}$ can be changed into

$$\begin{aligned}\dot{V}_{m,k} &\le \dot{V}_{m,k-1} + \vartheta_{m,k} z_{m,k}\alpha_{m,k} + \frac{1}{2}z^2_{m,k+1} - \frac{1}{2}z^2_{m,k} \\ &\quad + \vartheta_{m,k} z_{m,k} \frac{\hat{\lambda}_{m,k}\vartheta_{m,k} z_{m,k} H^{\mathrm{T}}_{p_{m,k}} H_{p_{m,k}}}{\sqrt{\vartheta^2_{m,k} z^2_{m,k} H^{\mathrm{T}}_{p_{m,k}} H_{p_{m,k}} + \Pi^2_{m,k}}} \\ &\quad + \vartheta_{m,k} z_{m,k} \frac{\hat{\Xi}_{m,k}\vartheta_{m,k} z_{m,k}}{\sqrt{\vartheta^2_{m,k} z^2_{m,k} + \Pi^2_{m,k}}} \\ &\quad + \Pi_{m,k}(\lambda_{m,k} + \Xi_{m,k}) \\ &\quad + \tilde{\lambda}_{m,k}(\tau_{m,k} - \dot{\hat{\lambda}}_{m,k}) + \tilde{\Xi}_{m,k}(\iota_{m,k} - \dot{\hat{\Xi}}_{m,k})\end{aligned} \tag{34}$$

where $\tau_{m,k} = \frac{\vartheta^2_{m,k} z^2_{m,k} H^{\mathrm{T}}_{p_{m,k}} H_{p_{m,k}}}{\sqrt{\vartheta^2_{m,k} z^2_{m,k} H^{\mathrm{T}}_{p_{m,k}} H_{p_{m,k}} + \Pi^2_{m,k}}}$, $\iota_{m,k} = \frac{\vartheta^2_{m,k} z^2_{m,k}}{\sqrt{\vartheta^2_{m,k} z^2_{m,k} + \Pi^2_{m,k}}}$.

According to the adaptive backstepping design process, the following virtual controller and adaptive laws are given

$$\begin{aligned}\alpha_{m,k} &= -\mu_{m,k} z_{m,k} - \frac{\vartheta_{m,k} z_{m,k}\hat{\Xi}_{m,k}}{\sqrt{\vartheta^2_{m,k} z^2_{m,k} + \Pi^2_{m,k}}} \\ &\quad - \frac{\vartheta_{m,k} z_{m,k}\hat{\lambda}_{m,k} H^{\mathrm{T}}_{p_{m,k}} H_{p_{m,k}}}{\sqrt{\vartheta^2_{m,k} z^2_{m,k} H^{\mathrm{T}}_{p_{m,k}} H_{p_{m,k}} + \Pi^2_{m,k}}}\end{aligned} \tag{35}$$

$$\dot{\hat{\lambda}}_{m,k} = \tau_{m,k} - \Pi_{m,k}\hat{\lambda}_{m,k} \tag{36}$$

$$\dot{\hat{\Xi}}_{m,k} = \iota_{m,k} - \Pi_{m,k}\hat{\Xi}_{m,k} \tag{37}$$

where $\mu_{m,k} > 0$ is the design parameter.

Then, integrating (34)–(37), $\dot{V}_{m,k}$ can be transformed as

$$\begin{aligned}\dot{V}_{m,k} &\le -\mu_{m,k}\vartheta_{m,k} z^2_{m,k} + \Pi_{m,k}(\lambda_{m,k} + \Xi_{m,k}) \\ &\quad + \Pi_{m,k}\tilde{\lambda}_{m,k}\hat{\lambda}_{m,k} + \Pi_{m,k}\tilde{\Xi}_{m,k}\hat{\Xi}_{m,k} \\ &\quad + \frac{1}{2}z^2_{m,k+1} - \frac{1}{2}z^2_{m,k} + \dot{V}_{m,k-1}\end{aligned} \tag{38}$$

In light of (25), $\dot{V}_{m,k}$ can be further changed into

$$\begin{aligned}\dot{V}_{m,k} &\le -\sum_{j=1}^{k}\mu_{m,j}\vartheta_{m,j} z^2_{m,j} + \sum_{j=1}^{k}\Pi_{m,j}(\lambda_{m,j} + \Xi_{m,j}) \\ &\quad + \sum_{j=1}^{k}\Pi_{m,j}\tilde{\lambda}_{m,j}\hat{\lambda}_{m,j} + \sum_{j=1}^{k}\Pi_{m,j}\tilde{\Xi}_{m,j}\hat{\Xi}_{m,j} \\ &\quad + \frac{1}{2}z^2_{m,k+1}\end{aligned} \tag{39}$$

Remark 8. $\frac{1}{2}z^2_{m,k+1}(k = 1,\ldots,n_m - 1)$ will be coped with in step $m,k+1$.

Step m,n_m: Similar to (13) and (26), the following Lyapunov function V_{m,n_m} is considered

$$V_{m,n_m} = V_{m,n_m-1} + V^{\iota}_{m,n_m} + \frac{1}{2}\tilde{\lambda}^2_{m,n_m} + \frac{1}{2}\tilde{\Xi}^2_{m,n_m} + \frac{\ell_{m,1}}{2}\tilde{\varsigma}^2_m \tag{40}$$

where $\lambda_{m,n_m} = \|\theta_{m,n_m}\|$ denotes unknown constant, θ_{m,n_m} is the weight vector of MTN. $\tilde{\lambda}_{m,n_m} = \lambda_{m,n_m} - \hat{\lambda}_{m,n_m}$ and $\hat{\lambda}_{m,n_m}$ is the estimation of λ_{m,n_m}. $\tilde{\lambda}_{m,n_m}$ is the estimation error. Similarly, $\tilde{\Xi}_{m,n_m} = \Xi_{m,n_m} - \hat{\Xi}_{m,n_m}$ is the estimation error with $\Xi_{m,n_m} = \bar{\Psi}_{m,n_m} + \bar{\phi}_{m,n_m} + \ell_{m,2}\varrho^*_m$, and $\tilde{\varsigma}_m = \varsigma_m - \hat{\varsigma}_m$ with $\varsigma_m = \frac{1}{\ell_{m,1}}$.

Denote $\pounds_{b_{m,n_m}} = \frac{z_{m,n_m}}{\varnothing_{b_{m,n_m}}}$ and $\vartheta_{m,n_m} = \frac{1}{\varnothing^2_{b_{m,n_m}} - z^2_{m,n_m}}$. Then, take the time derivative of V_{m,n_m}, one has

$$\begin{aligned}\dot{V}_{m,n_m} &= \dot{V}_{m,n_m-1} + \vartheta_{m,n_m} z_{m,n_m}\dot{z}_{m,n_m} \\ &\quad - \tilde{\lambda}_{m,n_m}\dot{\hat{\lambda}}_{m,n_m} - \tilde{\Xi}_{m,n_m}\dot{\hat{\Xi}}_{m,n_m} - \ell_{m,1}\tilde{\varsigma}_m\dot{\hat{\varsigma}}_m \\ &\quad - \left[\frac{\dot{\varnothing}_{b_{m,n_m}}}{\varnothing_{b_{m,n_m}}} \frac{\pounds_{b_{m,n_m}}}{\varnothing_{b_{m,n_m}}(1-\pounds^2_{b_{m,n_m}})}\right] z_{m,n_m}\end{aligned} \tag{41}$$

Then, based on (1) and (10), taking the time derivative of z_{m,n_m} produces

$$\dot{z}_{m,n_m} = u_m + \Gamma_{m,n_m} + \phi_{m,n_m} - \dot{\alpha}_{m,n_m-1} \tag{42}$$

Furthermore, combining (41) and (42), the time derivative of V_{m,n_m} becomes

$$\begin{aligned}\dot{V}_{m,n_m} &= \vartheta_{m,n_m} z_{m,n_m}(u_m + \tilde{\Gamma}_{m,n_m}) - \vartheta^2_{m,n_m} z^2_{m,n_m} \\ &\quad - \frac{1}{2}z^2_{m,n_m} + \vartheta_{m,n_m} z_{m,n_m}\phi_{m,n_m} - \tilde{\lambda}_{m,n_m}\dot{\hat{\lambda}}_{m,n_m} \\ &\quad - \tilde{\Xi}_{m,n_m}\dot{\hat{\Xi}}_{m,n_m} - \ell_{m,1}\tilde{\varsigma}_m\dot{\hat{\varsigma}}_m + \dot{V}_{m,n_m-1}\end{aligned} \tag{43}$$

where $\tilde{\Gamma}_{m,n_m} = \Gamma_{m,n_m} - \dot{\alpha}_{m,n_m-1} - \frac{1}{\vartheta_{m,n_m}} \frac{\dot{\varnothing}_{b_{m,n_m}}}{\varnothing_{b_{m,n_m}}} \frac{\pounds_{b_{m,n_m}}}{\varnothing_{b_{m,n_m}}(1-\pounds^2_{b_{m,n_m}})} + \vartheta_{m,n_m} z_{m,n_m} + \frac{1}{2\vartheta_{m,n_m}} z_{m,n_m}$ is a combination of nonlinear functions. Based on the MTN approximation technique in Lemma 1, for any constant $\bar{\Psi}_{m,n_m} > 0$, $\tilde{\Gamma}_{m,n_m}$

can be approximated by one MTN, that is, the following formula can be established

$$\tilde{\Gamma}_{m,n_m} = \theta^{\mathrm{T}}_{m,n_m} H_{p_{m,n_m}} + \Psi_{m,n_m}, \left|\Psi_{m,n_m}\right| \le \bar{\Psi}_{m,n_m} \tag{44}$$

where Ψ_{m,n_m} is the approximation error of the combination term $\tilde{\Gamma}_{m,n_m}$ and $\theta^{\mathrm{T}}_{m,n_m} H_{p_{m,n_m}}$.

Then, substituting (44) into (43) along with taking (2) and (10) into account, it can be obtained that

$$\begin{aligned}\dot{V}_{m,n_m} &= \ell_{m,1}\vartheta_{m,n_m} z_{m,n_m} \upsilon_m + \vartheta_{m,n_m} z_{m,n_m} \theta^{\mathrm{T}}_{m,n_m} H_{p_{m,n_m}} \\ &+ \vartheta_{m,n_m} z_{m,n_m} (\phi_{m,n_m} + \Psi_{m,n_m} + \ell_{m,2}\varrho_m) \\ &- \vartheta^2_{m,n_m} z^2_{m,n_m} - \frac{1}{2} z^2_{m,n_m} - \tilde{\Xi}_{m,n_m}\dot{\hat{\Xi}}_{m,n_m} \\ &- \ell_{m,1}\tilde{\varsigma}_m\dot{\hat{\varsigma}}_m + \dot{V}_{m,n_m-1}\end{aligned} \tag{45}$$

Similar to (19) in step $m,1$, (32) in step m,k and taking (2), (5) into account, one has

$$\begin{aligned}&\vartheta_{m,n_m} z_{m,n_m} \theta^{\mathrm{T}}_{m,n_m} H_{p_{m,n_m}} \\ &+ \vartheta_{m,n_m} z_{m,n_m} (\Psi_{m,n_m} + \phi_{m,n_m} + \ell_{m,2}\varrho_m) \\ &\le \frac{\lambda_{m,n_m}\vartheta^2_{m,n_m} z^2_{m,n_m} H^{\mathrm{T}}_{p_{m,n_m}} H_{p_{m,n_m}}}{\sqrt{\vartheta^2_{m,n_m} z^2_{m,n_m} H^{\mathrm{T}}_{p_{m,n_m}} H_{p_{m,n_m}} + \Pi^2_{m,n_m}}} \\ &+ \frac{\Xi_{m,n_m}\vartheta^2_{m,n_m} z^2_{m,n_m}}{\sqrt{\vartheta^2_{m,n_m} z^2_{m,n_m} + \Pi^2_{m,n_m}}} + \Xi_{m,n_m}\Pi_{m,n_m} \\ &+ \lambda_{m,n_m}\Pi_{m,n_m}\end{aligned} \tag{46}$$

Then, substituting (46) into (45), the time derivative of V_{m,n_m} can be recomputed as

$$\begin{aligned}\dot{V}_{m,n_m} &\le \ell_{m,1}\vartheta_{m,n_m} z_{m,n_m} \upsilon_m + \Pi_{m,n_m}(\lambda_{m,n_m} + \Xi_{m,n_m}) \\ &+ \frac{\hat{\lambda}_{m,n_m}\vartheta^2_{m,n_m} z^2_{m,n_m} H^{\mathrm{T}}_{p_{m,n_m}} H_{p_{m,n_m}}}{\sqrt{\vartheta^2_{m,n_m} z^2_{m,n_m} H^{\mathrm{T}}_{p_{m,n_m}} H_{p_{m,n_m}} + \Pi^2_{m,n_m}}} \\ &+ \frac{\hat{\Xi}_{m,n_m}\vartheta^2_{m,n_m} z^2_{m,n_m}}{\sqrt{\vartheta^2_{m,n_m} z^2_{m,n_m} + \Pi^2_{m,n_m}}} - \frac{1}{2} z^2_{m,n_m} \\ &+ \tilde{\lambda}_{m,n_m}(\tau_{m,n_m} - \dot{\hat{\lambda}}_{m,n_m}) + \tilde{\Xi}_{m,n_m}(\iota_{m,n_m} - \dot{\hat{\Xi}}_{m,n_m}) \\ &- \ell_{m,1}\tilde{\varsigma}_m\dot{\hat{\varsigma}}_m + \dot{V}_{m,n_m-1}\end{aligned} \tag{47}$$

where $\tau_{m,n_m} = \frac{\vartheta^2_{m,n_m} z^2_{m,n_m} H^{\mathrm{T}}_{p_{m,n_m}} H_{p_{m,n_m}}}{\sqrt{\vartheta^2_{m,n_m} z^2_{m,n_m} H^{\mathrm{T}}_{p_{m,n_m}} H_{p_{m,n_m}} + \Pi^2_{m,n_m}}}$, $\iota_{m,n_m} = \frac{\vartheta^2_{m,n_m} z^2_{m,n_m}}{\sqrt{\vartheta^2_{m,n_m} z^2_{m,n_m} + \Pi^2_{m,n_m}}}$.

Similar to step $m,1$, the following virtual controller and adaptive laws are given

$$\begin{aligned}\alpha_{m,n_m} &= -\mu_{m,n_m} z_{m,n_m} - \frac{\vartheta_{m,n_m} z_{m,n_m}\hat{\Xi}_{m,n_m}}{\sqrt{\vartheta^2_{m,n_m} z^2_{m,n_m} + \Pi^2_{m,n_m}}} \\ &- \frac{\vartheta_{m,n_m} z_{m,n_m}\hat{\lambda}_{m,n_m} H^{\mathrm{T}}_{p_{m,n_m}} H_{p_{m,n_m}}}{\sqrt{\vartheta^2_{m,n_m} z^2_{m,n_m} H^{\mathrm{T}}_{p_{m,n_m}} H_{p_{m,n_m}} + \Pi^2_{m,n_m}}}\end{aligned} \tag{48}$$

$$\upsilon_m = \hat{\varsigma}_m \alpha_{m,n_m} \tag{49}$$

$$\dot{\hat{\lambda}}_{m,n_m} = \tau_{m,n_m} - \Pi_{m,n_m}\hat{\lambda}_{m,n_m} \tag{50}$$

$$\dot{\hat{\Xi}}_{m,n_m} = \iota_{m,n_m} - \Pi_{m,n_m}\hat{\Xi}_{m,n_m} \tag{51}$$

$$\dot{\hat{\varsigma}}_m = -\vartheta_{m,n_m} z_{m,n_m}\alpha_{m,n_m} - \Pi_{m,n_m}\hat{\varsigma}_m \tag{52}$$

where $\mu_{m,n_m} > 0$ is the design parameter.

Remark 9. Different from the method of directly approximating the unknown hysteresis parameter $\ell_{m,1}$ in Li et al. (2012), this paper approximates the new intermediate variable $\varsigma_m = \frac{1}{\ell_{m,1}}$ and further adds a new adaptive law, which makes the difficulty caused by the unknown hysteresis input settled. It should be emphasized that the problem of the denominator to be zero may occur by the method in Li et al. (2012). On the contrary, it can be seen from (49) that the method proposed in this paper can avoid the above "singularity" problem.

Then, integrating (47) to (52), the time derivative of V_{m,n_m} can be transformed as

$$\begin{aligned}\dot{V}_{m,n_m} &\le \ell_{m,1}\vartheta_{m,n_m} z_{m,n_m}\varsigma_m\alpha_{m,n_m} + \Pi_{m,n_m}(\lambda_{m,n_m} + \Xi_{m,n_m}) \\ &+ \frac{\hat{\lambda}_{m,n_m}\vartheta^2_{m,n_m} z^2_{m,n_m} H^{\mathrm{T}}_{p_{m,n_m}} H_{p_{m,n_m}}}{\sqrt{\vartheta^2_{m,n_m} z^2_{m,n_m} H^{\mathrm{T}}_{p_{m,n_m}} H_{p_{m,n_m}} + \Pi^2_{m,n_m}}} \\ &+ \frac{\hat{\Xi}_{m,n_m}\vartheta^2_{m,n_m} z^2_{m,n_m}}{\sqrt{\vartheta^2_{m,n_m} z^2_{m,n_m} + \Pi^2_{m,n_m}}} - \frac{1}{2} z^2_{m,n_m} \\ &+ \Pi_{m,n_m}\tilde{\lambda}_{m,n_m}\hat{\lambda}_{m,n_m} + \Pi_{m,n_m}\tilde{\Xi}_{m,n_m}\hat{\Xi}_{m,n_m} \\ &+ \Pi_{m,n_m}\ell_{m,1}\tilde{\varsigma}_m\hat{\varsigma}_m + \dot{V}_{m,n_m-1} \\ &= -\mu_{m,n_m}\vartheta_{m,n_m} z^2_{m,n_m} + \Pi_{m,n_m}\tilde{\Xi}_{m,n_m}\hat{\Xi}_{m,n_m} \\ &+ \Pi_{m,n_m}(\lambda_{m,n_m} + \Xi_{m,n_m}) + \Pi_{m,n_m}\tilde{\lambda}_{m,n_m}\hat{\lambda}_{m,n_m} \\ &- \frac{1}{2} z^2_{m,n_m} + \ell_{m,1}\Pi_{m,n_m}\tilde{\varsigma}_m\hat{\varsigma}_m + \dot{V}_{m,n_m-1}\end{aligned} \tag{53}$$

Based on $\vartheta_{m,j} = \frac{1}{\emptyset^2_{b_{m,j}} - z^2_{m,j}}$ and $z_{m,j} \in \Omega_z := \{z_{m,j} \in R, \left|z_{m,j}\right| < \emptyset_{b_{i,j}}\}$, the time derivative of V_{m,n_m} can be further transformed as

$$\begin{aligned}\dot{V}_{m,n_m} &\le -\sum_{j=1}^{n_m}\mu_{m,j}\vartheta_{m,j} z^2_{m,j} + \sum_{j=1}^{n_m}\Pi_{m,j}(\lambda_{m,j} + \Xi_{m,j}) \\ &+ \sum_{j=1}^{n_m}\Pi_{m,j}\tilde{\lambda}_{m,j}\hat{\lambda}_{m,j} + \sum_{j=1}^{n_m}\Pi_{m,j}\tilde{\Xi}_{m,j}\hat{\Xi}_{m,j} \\ &+ \ell_{m,1}\Pi_{m,n_m}\tilde{\varsigma}_m\hat{\varsigma}_m \\ &= -\sum_{j=1}^{n_m}\mu_{m,j}\left(\frac{z^2_{m,j}}{\emptyset^2_{b_{m,j}} - z^2_{m,j}}\right) + \sum_{j=1}^{n_m}\Pi_{m,j}\tilde{\lambda}_{m,j}\hat{\lambda}_{m,j} \\ &+ \sum_{j=1}^{n_m}\Pi_{m,j}(\lambda_{m,j} + \Xi_{m,j}) + \sum_{j=1}^{n_m}\Pi_{m,j}\tilde{\Xi}_{m,j}\hat{\Xi}_{m,j} \\ &+ \ell_{m,1}\Pi_{m,n_m}\tilde{\varsigma}_m\hat{\varsigma}_m\end{aligned} \tag{54}$$

Then, applying Lemma 5, the time derivative of V_{m,n_m} can be further obtained

$$\begin{aligned}\dot{V}_{m,n_m} &\le -\sum_{j=1}^{n_m}\mu_{m,j}\ln\left(\frac{\emptyset^2_{b_{m,j}}}{\emptyset^2_{b_{m,j}} - z^2_{m,j}}\right) \\ &+ \sum_{j=1}^{n_m}\Pi_{m,j}\tilde{\lambda}_{m,j}\hat{\lambda}_{m,j} + \sum_{j=1}^{n_m}\Pi_{m,j}(\lambda_{m,j} + \Xi_{m,j}) \\ &+ \sum_{j=1}^{n_m}\Pi_{m,j}\tilde{\Xi}_{m,j}\hat{\Xi}_{m,j} + \ell_{m,1}\Pi_{m,n_m}\tilde{\varsigma}_m\hat{\varsigma}_m\end{aligned} \tag{55}$$

Now, the design of the controller has been completed using the backstepping method.

3.2. Stability analysis

In this part, the stability analysis is given by Lyapunov stability and Lemma 3, which is also a proof of the efficiency of the design algorithm in Section 3.1. The main results are summarized by the following Theorem 1.

Theorem 1. *Considering nonlinear MIMO systems (1) with time-varying full-state constraints and input hysteresis under Assumptions 1–2, if the actual controller (49), the virtual control signals (22), (35), (48) and adaptive laws (23),(24), (36),(37), (50)–(52) are selected, then the proposed controller can achieve the following goals:*

(1) the tracking error can converge to zero asymptotically, i.e., $\lim_{t\to\infty} z_{m,1} = 0$;
(2) all signals of the closed-loop system remain bounded;
(3) all states of the system are within the given time-varying constraints.

Proof. According to Lemma 4, the following inequalities hold

$$\tilde{\lambda}_{m,j}\hat{\lambda}_{m,j} \le -\tilde{\lambda}_{m,j}^2 + \tilde{\lambda}_{m,j}\lambda_{m,j} \le \frac{1}{4}\lambda_{m,j}^2 \tag{56}$$

$$\tilde{\Xi}_{m,j}\hat{\Xi}_{m,j} \le -\tilde{\Xi}_{m,j}^2 + \tilde{\Xi}_{m,j}\Xi_{m,j} \le \frac{1}{4}\Xi_{m,j}^2 \tag{57}$$

$$\tilde{\varsigma}_m\hat{\varsigma}_m \le -\tilde{\varsigma}_m^2 + \tilde{\varsigma}_m\varsigma_m \le \frac{1}{4}\varsigma_m^2 \tag{58}$$

Then, combining (56)–(58), the time derivative of V_{m,n_m} can be further obtained

$$\begin{aligned}\dot{V}_{m,n_m} \le& -\sum_{j=1}^{n_m}\mu_{m,j}\ln\left(\frac{\O_{b_{m,j}}^2}{\O_{b_{m,j}}^2 - z_{m,j}^2}\right)\\ &+ \frac{1}{4}\sum_{j=1}^{n_m}\Pi_{m,j}\lambda_{m,j}^2 + \sum_{j=1}^{n_m}\Pi_{m,j}(\lambda_{m,j} + \Xi_{m,j})\\ &+ \frac{1}{4}\sum_{j=1}^{n_m}\Pi_{m,j}\Xi_{m,j}^2 + \frac{1}{4}\ell_{m,1}\Pi_{m,n_m}\varsigma_m^2\\ \le& -\sum_{j=1}^{n_m}\mu_{m,j}\ln\left(\frac{\O_{b_{m,j}}^2}{\O_{b_{m,j}}^2 - z_{m,j}^2}\right) + \sum_{j=1}^{n_m}\eta_{m,j}\Pi_{m,j}\end{aligned} \tag{59}$$

where $\eta_{m,j} = \lambda_{m,j} + \Xi_{m,j} + \frac{1}{4}\lambda_{m,j}^2 + \frac{1}{4}\Xi_{m,j}^2 (m = 1,\ldots,n, j = 1,\ldots,n_m - 1)$, $\eta_{m,n_m} = \lambda_{m,n_m} + \Xi_{m,n_m} + \frac{1}{4}\lambda_{m,n_m}^2 + \frac{1}{4}\Xi_{m,n_m}^2 + \frac{\ell_{m,1}}{4}\varsigma_m^2$.

Remark 10. The design parameter $\mu_{m,j}$ is introduced to ensure that the controller can achieve more accurate tracking performance. Moreover, by defining $\lambda_{m,j} = \left\|\theta_{m,j}\right\|$ to estimate the norm of $\theta_{m,j}$ rather than themselves, the computational burden of controller is greatly reduced. According to the controller design process, design the Lyapunov function V for the closed-loop system as $V = V_{m,n_m}$.

Therefore, based on (55), one has

$$\dot{V} \le \sum_{m=1}^{n}\left[-\sum_{j=1}^{n_m}\mu_{m,j}\ln\left(\frac{\O_{b_{m,j}}^2}{\O_{b_{m,j}}^2 - z_{m,j}^2}\right) + \sum_{j=1}^{n_m}\eta_{m,j}\Pi_{m,j}\right] \tag{60}$$

According to Lemma 2, integrating (60) with respect to t from t_0 to t and taking the known constraints $\left|z_{m,j}\right| < \O_{b_{m,j}}$ into account, one has

$$\begin{aligned}V \le& V(t_0) - \sum_{m=1}^{n}\sum_{j=1}^{n_m}\mu_{m,j}\int_{t_0}^{t}\ln\left(\frac{\O_{b_{m,j}}^2}{\O_{b_{m,j}}^2 - z_{m,j}^2}\right)d\epsilon\\ &+ \sum_{m=1}^{n}\sum_{j=1}^{n_m}\eta_{m,j}\int_{t_0}^{t}\Pi_{m,j}d\tau\\ \le& V(t_0) + \sum_{m=1}^{n}\sum_{j=1}^{n_m}\eta_{m,j}\bar{\Pi}_{m,j}\end{aligned} \tag{61}$$

(i) According to (61), $z_{m,j}$, $\tilde{\lambda}_{m,j}$, $\tilde{\Xi}_{m,j}$ and $\tilde{\varsigma}_m$ are bounded with $\left|z_{m,1}\right| < \O_{b_{m,1}}$. Furthermore, it can be concluded that $\hat{\lambda}_{m,j}$, $\hat{\Xi}_{m,j}$ and $\hat{\varsigma}_m$ are bounded. Therefore, based on $z_{m,1} = \chi_{m,1} - y_{m,r}$ and the boundedness of $y_{m,r}$, it can be concluded that $\chi_{m,1}$ is bounded. In addition, it can be deduced from (22) that $\alpha_{m,1}$ is bounded. Then, since $z_{m,2} = \chi_{m,2} - \alpha_{m,1}$, $\chi_{m,2}$ is bounded. And so on to conclude that all signals of the closed-loop system are bounded.

(ii) It can be concluded from Assumption 1 that $\left|\chi_{m,1}\right| \le \left|z_{m,1}\right| + \left|y_{m,r}\right| < \O_{b_{m,1}}(t) + \bar{A}_{m,0} = \O_{c_{m,1}}(t)$, i.e., $\left|\chi_{m,1}\right| \le \O_{c_{m,1}}(t)$. Next, because $\left|\alpha_{m,1}\right| < \Lambda_{m,1}(t)$, $\left|\chi_{m,2}\right| \le \left|z_{m,2}\right| + \left|\alpha_{m,1}\right| < \O_{b_{m,2}}(t) + \Lambda_{m,1}(t) = \O_{c_{m,2}}(t)$ holds,

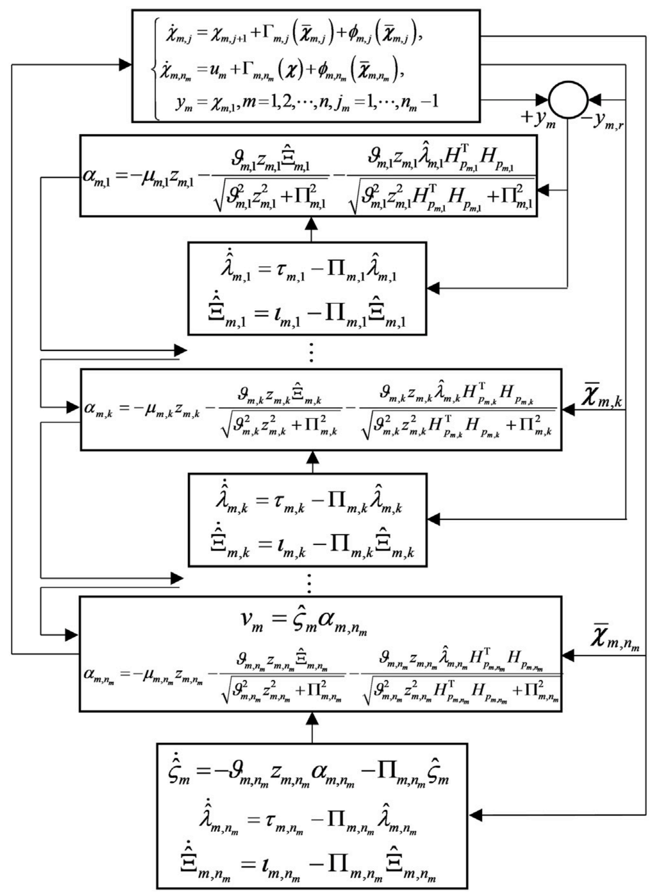

Fig. 2. The system control block diagram.

i.e., $\left|\chi_{m,2}\right| \le \O_{c_{m,2}}(t)$. Similarly, $\left|\chi_{m,j}\right| \le \O_{c_{m,j}}(t)$, which means that the time-varying full-state constraints are not violated.

(iii) In addition, according to (15) and the boundedness of all signals, $\dot{z}_{m,1}$ is bounded. Therefore, it can be further to know $z_{m,1}$ is uniformly continuous. Then, by applying Lemma 3, we can conclude that $\lim_{t\to\infty} z_{m,1}(t) = 0, m = 1,\ldots,n$, that is, the tracking error can converge to zero asymptotically.

Remark 11. $\Pi_{m,j}$ is introduced to ensure asymptotic tracking effect, while $\mu_{m,j}$ is added to ensure the better tracking performance. In theory, we can increase $\mu_{m,j}$ and $\Pi_{m,j}$ arbitrarily. However, from (22), (35), and (48), increasing $\mu_{m,j}$ or decreasing $\Pi_{m,j}$ may increase the amplitude of control signals. So, there should be a tradeoff between tracking performance and control effort to ensure better control performance.

Remark 12. In this paper, the robustness against approximation errors, external disturbances, and the hysteresis nonlinearity can be guaranteed by constructing the adaptive laws (24), (37) and (51) to approximate the upper bound of the disturbance-like terms containing approximation errors $\Psi_{m,j}$, external disturbances $\phi_{m,j}$, and the bounded terms ϱ_m of the hysteresis model. Meanwhile, it is essential that by introducing positive continuous functions $\Pi_{m,j}$ into adaptive laws and controllers, the high-precision asymptotic tracking control effect can be realized.

Remark 13. Figs. 2 and 3 illustrate the system control block diagram and the algorithm mechanism flow, respectively.

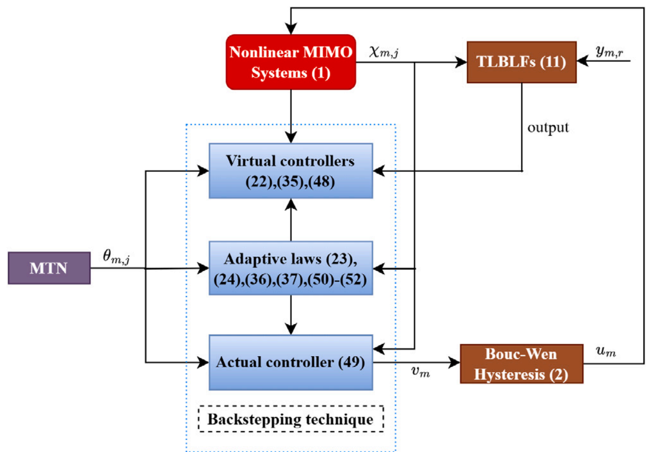

Fig. 3. The flowchart of the control algorithm in this paper.

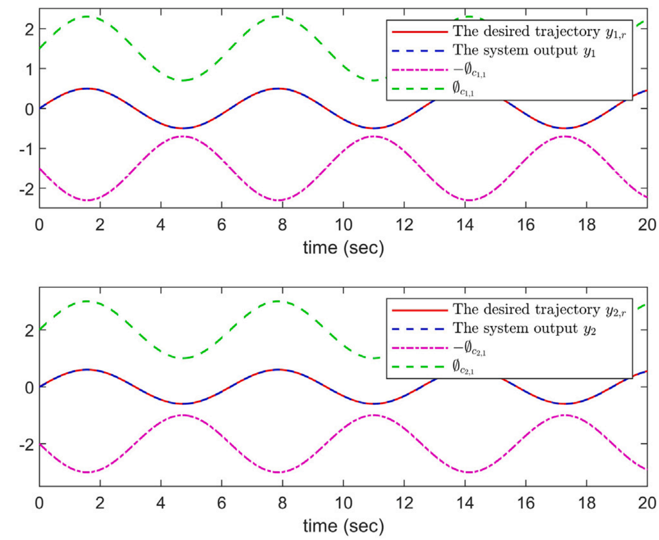

Fig. 4. The tracking effect with constraints in Example 1.

Table 1
Design parameters of system (62).

Parameter	Value
The initial state of the controlled system	$\chi_1(\mathbf{0}) = \chi_2(\mathbf{0}) = [0, 0]^{\mathrm{T}}$
Reference signals	$y_{1,r} = 0.5\sin t,\ y_{2,r} = 0.6\sin t$
The positive continuous functions	$\Pi_{1,1} = 0.002e^{-0.01t}, \Pi_{1,2} = 0.001e^{-0.01t}, \Pi_{2,1} = \Pi_{2,2} = 0.0015e^{-0.01t}$
Controller parameters	$\mu_{1,1} = \mu_{1,2} = \mu_{2,1} = \mu_{2,2} = 5$
Bouc–Wen hysteresis parameters	$\iota = 1.2, \bar{\varphi} = 1, \kappa = 3, \ell_{m,1} = 3, \ell_{m,2} = 2$

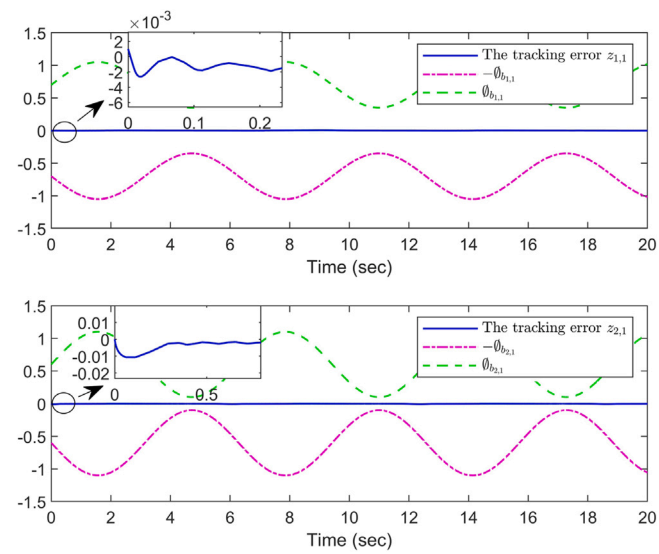

Fig. 5. The tracking error trajectory with constraints in Example 1.

4. Simulation results

In order to verify the validity of the proposed control strategy, a numerical simulation, a practical simulation based on the inverted double pendulums and a comparison test are accomplished in Example 1, Example 2 and Example 3, respectively.

Example 1. Considering the following MIMO nonlinear systems with input hysteresis to verify the validity of the proposed scheme.

$$\begin{cases} \dot{\chi}_{1,1} = \chi_{1,2} + \Gamma_{1,1} + \phi_{1,1} \\ \dot{\chi}_{1,2} = u_1 + \Gamma_{1,2} + \phi_{1,2} \\ \ y_1 = \chi_{1,1} \\ \dot{\chi}_{2,1} = \chi_{2,2} + \Gamma_{2,1} + \phi_{2,1} \\ \dot{\chi}_{2,2} = u_2 + \Gamma_{2,2} + \phi_{2,2} \\ \ y_2 = \chi_{2,1} \end{cases} \tag{62}$$

where $\Gamma_{1,1} = 0.02\sin(\chi_{1,1})$, $\Gamma_{1,2} = 0.1\chi_{1,2}\cos(\chi_{1,1})$, $\Gamma_{2,1} = 0.5\sin(\chi_{2,1})$, $\Gamma_{2,2} = -0.1\chi_{1,1}^2\chi_{2,2}\cos(\chi_{2,1})$, $\phi_{1,1} = 0.2\cos^2(\chi_{1,1})$, $\phi_{1,2} = -0.1\sin(2\chi_{1,2})\cos(\chi_{1,1})$, $\phi_{2,1} = -0.2\cos^2(\chi_{2,1})$, $\phi_{2,2} = 0$. $u_m(i = 1, 2)$ is the system input constrained by hysteresis which is defined as (2). The constraints are specified as $\emptyset_{c_{1,1}} = 0.8\sin t + 1.5$, $\emptyset_{c_{1,2}} = \sin t + 0.8$, $\emptyset_{c_{2,1}} = \sin t + 2$, $\emptyset_{c_{2,2}} = 1.5\sin t + 2.3$. And the design parameters are selected as $\emptyset_{b_{1,1}} = 0.35\sin t + 0.7$, $\emptyset_{b_{1,2}} = 0.5\sin t + 1.1$, $\emptyset_{b_{2,1}} = 0.5\sin t + 0.6$, $\emptyset_{b_{2,2}} = 0.4\sin t + 1$.

In simulation, the initial conditions are given as $\chi_{1,1}(0) = \chi_{1,2}(0) = \chi_{2,1}(0) = \chi_{2,2}(0) = 0$. The design parameters of the control structure are presented in Table 1.

In the simulation part, the positive continuous function $\Pi_{m,j}$ is designed as an exponential function form. It should be noted that positive continuous functions in the form of exponential functions are commonly found in many literatures about asymptotic tracking control, such as Du et al. (2023), Li et al. (2022a), Wu et al. (2023).

The corresponding simulation results are shown in Figs. 4–7. The system output y_m and the desired signal $y_{m,r}$ under the time-varying constraints are displayed in Fig. 4. It is obvious that despite giving different desired trajectories, the proposed strategy can ensure the system output track the reference signal which can be observed from Fig. 5. Fig. 6 shows the trajectory of system states. Apparently, full-state constraints are not violated. Fig. 7 shows that hysteresis input, output and disturbance items are bounded. As the above figures show, all signals of the closed-loop system are bounded.

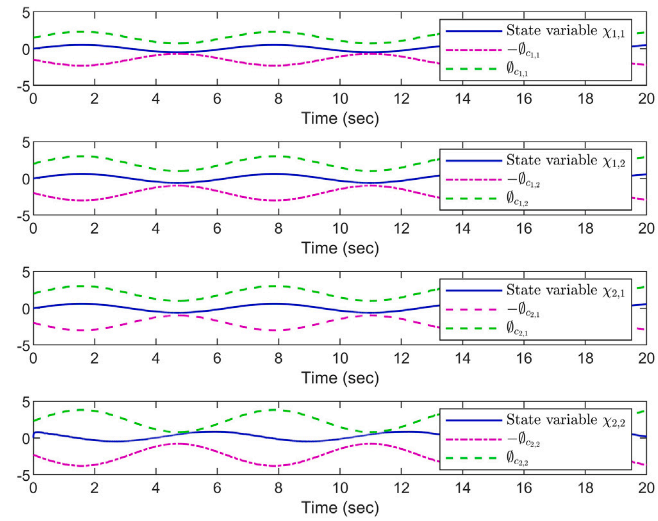

Fig. 6. The system states with time-varying constraints in Example 1.

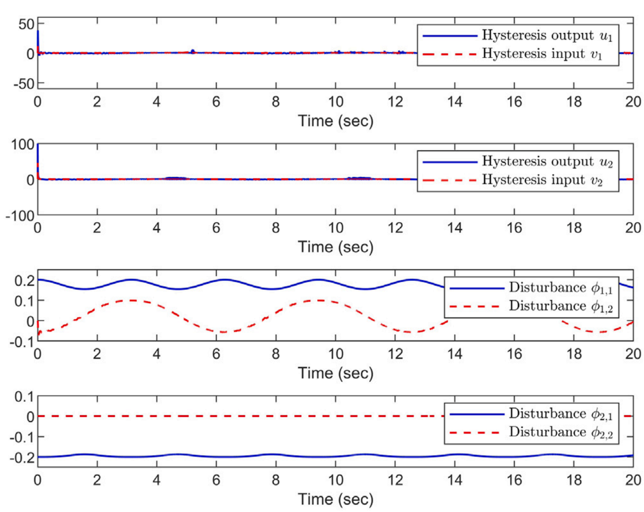

Fig. 7. Hysteresis output, input and disturbance items in Example 1.

Example 2. This example takes the inverted double pendulums (Bikas & Rovithakis, 2019) as the object to study the effectiveness of the proposed controller. The dynamics model of the inverted double pendulums is as follows

$$\begin{cases} \ddot{\theta}_1 = (\frac{m_1 g h}{T_1} - \frac{l h^2}{4T_1})\sin(\theta_1) + \frac{u_1}{T_1} \\ \quad + \frac{lh}{2T_1}(w-q) + \frac{lh^2}{4T_1}\sin(\dot{\theta}_2) \\ \ddot{\theta}_2 = (\frac{m_2 g h}{T_2} - \frac{l h^2}{4T_2})\sin(\theta_2) + \frac{u_2}{T_2} \\ \quad + \frac{lh}{2T_2}(w-q) + \frac{lh^2}{4T_2}\sin(\dot{\theta}_1) \end{cases} \tag{63}$$

Table 2
Design parameters of system (64).

Parameter	Value
The initial state of the controlled system	$\chi_1(\mathbf{0}) = \chi_2(\mathbf{0}) = [0,0]^{\mathrm{T}}$
Reference signals	$y_{1,r} = 0.5\sin t,\ y_{2,r} = 0.6\sin t$
The positive continuous functions	$\Pi_{1,1} = \Pi_{1,2} = 0.002e^{-0.01t}, \Pi_{2,1} = \Pi_{2,2} = 0.002e^{-0.01t}$
Controller parameters	$\mu_{1,1} = \mu_{1,2} = \mu_{2,1} = \mu_{2,2} = 5$
Bouc–Wen hysteresis parameters	$\imath = 1.2, \bar{\varphi} = 1, \kappa = 3, \ell_{m,1} = 3, \ell_{m,2} = 2$

Table 3
The parameters of system (63).

Parameters	Description	Value	Unit
m_1, m_2	the pendulum mass	1	kg
T_1, T_2	the moment of inertia	1	kg
h	the pendulum height	0.1	m
g	the gravity acceleration	9.8	m/s^2
l	the spring coefficient	10	N/m
w	the spring length	0.5	m
q	the distance between the pendulum hinges	0.4	m

where θ_m and $\dot{\theta}_m$ are the angular position and the angular velocity, respectively. Then, denote $\chi_{1,1} = \theta_1$, $\chi_{1,2} = \dot{\theta}_1$, $\chi_{2,1} = \theta_2$, $\chi_{2,2} = \dot{\theta}_2$, system (63) can be rewritten as

$$\begin{cases} \dot{\chi}_{1,1} = \chi_{1,2} \\ \dot{\chi}_{1,2} = \frac{1}{T_1}u_1 + \Gamma_{1,2} \\ \quad y_1 = \chi_{1,1} \\ \dot{\chi}_{2,1} = \chi_{2,2} \\ \dot{\chi}_{2,2} = \frac{1}{T_2}u_2 + \Gamma_{2,2} \\ \quad y_2 = \chi_{2,1} \end{cases} \tag{64}$$

with $\Gamma_{1,2} = (\frac{m_1 g h}{T_1} - \frac{lh^2}{4T_1})\sin(\chi_{1,1}) + \frac{lh^2}{4T_1}\sin(\chi_{2,2}) + \frac{lh}{2T_1}(w-q)$, $\Gamma_{2,2} = (\frac{m_2 g h}{T_2} - \frac{lh^2}{4T_2})\sin(\chi_{2,1}) + \frac{lh^2}{4T_1}\sin(\chi_{1,2}) + \frac{lh}{2T_2}(w-q)$, $\Gamma_{1,1} = \Gamma_{2,1} = \phi_{1,1} = \phi_{1,2} = \phi_{2,1} = \phi_{2,2} = 0$. $u_m (i = 1, 2)$ is the input of the system which is defined as (2). The constraints are specified as $\emptyset_{c_{1,1}} = 0.8\sin t + 1.5$, $\emptyset_{c_{1,2}} = \sin t + 0.8$, $\emptyset_{c_{2,1}} = \sin t + 2$, $\emptyset_{c_{2,2}} = 1.5\sin t + 1.9$. Therefore, the design parameters are selected as $\emptyset_{b_{1,1}} = 0.35\sin t + 0.7$, $\emptyset_{b_{1,2}} = 0.5\sin t + 1.1$, $\emptyset_{b_{2,1}} = 0.5\sin t + 0.6$, $\emptyset_{b_{2,2}} = 0.4\sin t + 1$.

Table 2 and Table 3 present the design parameters of the controller and the inverted double pendulums, respectively.

The corresponding simulation results are exhibited in Figs. 8–11. The system output y_m and the desired signal $y_{m,r}$ under the time-varying constraints are displayed in Fig. 8. It is clearly seen from Fig. 9 that the proposed scheme achieve a satisfactory tracking effect. Fig. 10 shows the system states are within the time-varying constraints boundary. Fig. 11 shows that both hysteresis input and output are bounded. All results indicate that the designed controller is effective for the inverted double pendulums.

Example 3. To underscore the superiority of the control scheme based on MTN approximation technology in this paper, a comparative test has been set based on Example 2, which involves evaluating the tracking performance of the MTN-based scheme proposed in this paper against the RBFNN-based control scheme proposed in Deng et al. (2022), Li and Li (2021), Zhu et al. (2023).

As depicted in Fig. 12, both control schemes exhibit good tracking performance. Nevertheless, the MTNs-based control scheme proposed in this paper generally displays a superior tracking effect compared to the RBFNNs-based control scheme. This further implies the superiority of the control scheme put forth in this paper.

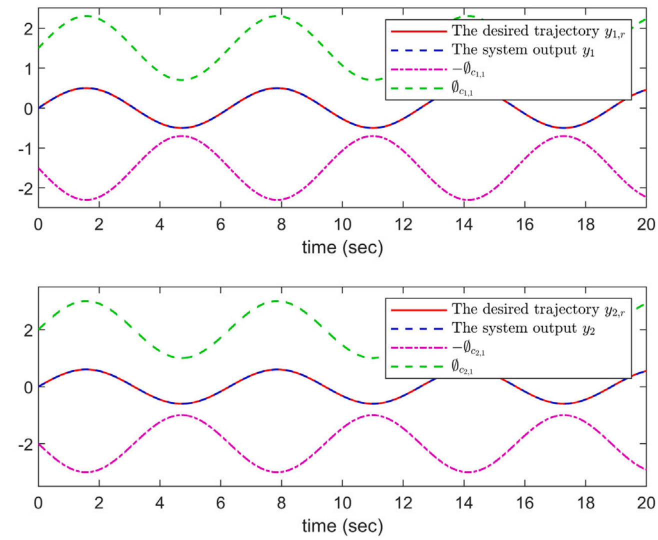

Fig. 8. The tracking effect with constraints in Example 2.

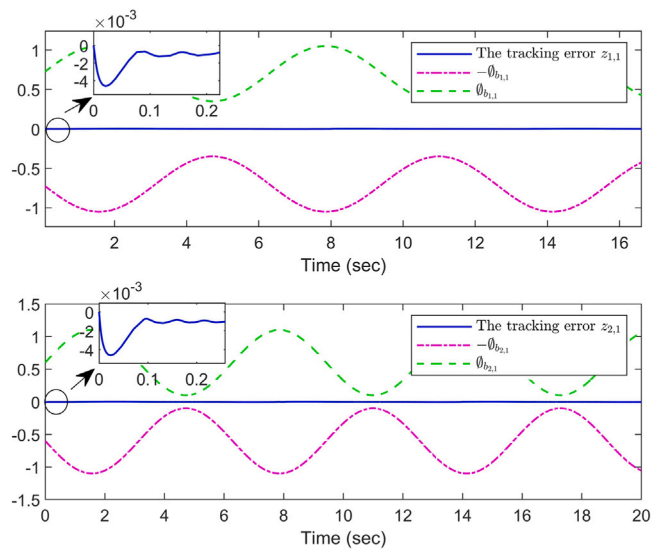

Fig. 9. The tracking error trajectory with constraints in Example 2.

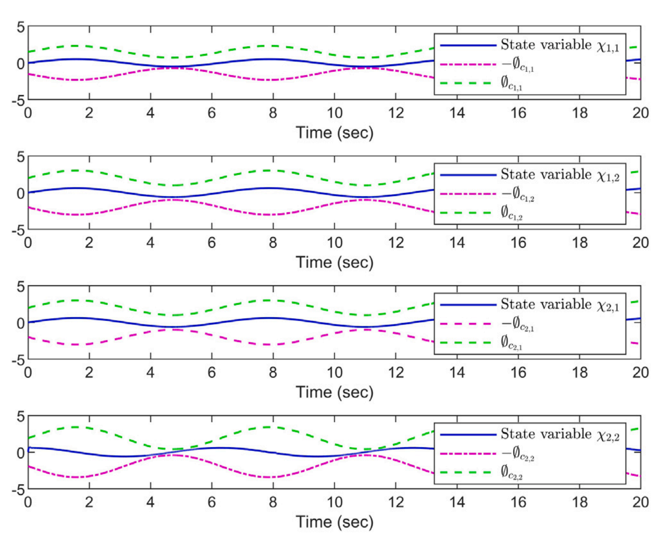

Fig. 10. The system states with time-varying constraints in Example 2.

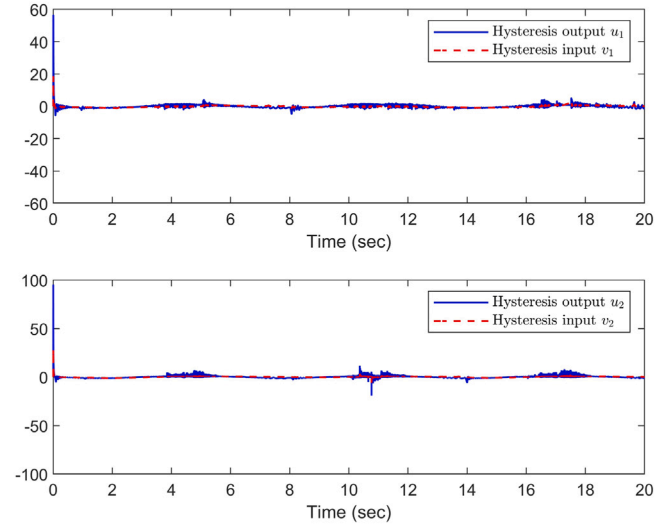

Fig. 11. Hysteresis output and input in Example 2.

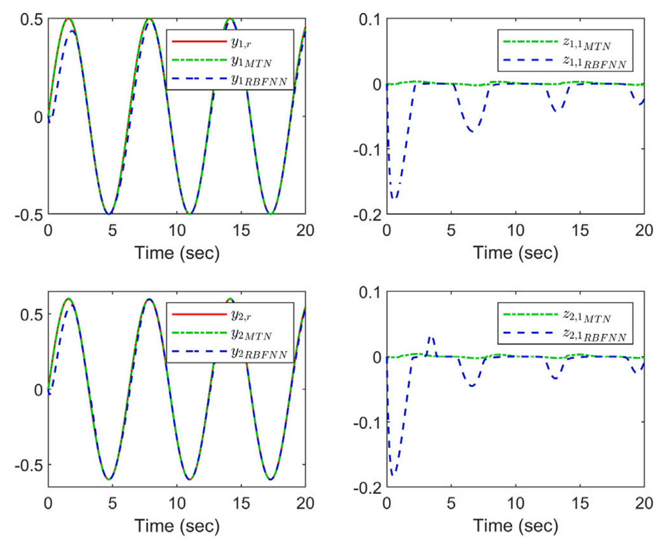

Fig. 12. Tracking effect comparison of two different scheme in Example 3.

5. Conclusion

In this paper, the asymptotic tracking control issue for nonlinear MIMO systems with time-varying full-state constraints and unknown hysteresis input is investigated. Firstly, by introducing new positive continuous functions, adaptive laws concerning the disturbance-like terms are designed to achieve excellent asymptotic tracking performance. To address the issue of hysteresis input, an adaptive law is added by approximating a new variable, which not only reduces the hysteresis effect but also avoids the "singularity" problem. In addition, time-varying full-state constraints are handled by using TLBLFs which ensure that all states of the controlled system stay within the constraint range. Finally, the simulations show the superiority of the proposed MTN-based control method in guaranteeing asymptotic tracking performance. Future research could explore the implementation of adaptive tracking control for nonlinear systems under deception attacks, with a novel hysteresis model proposed to characterize the hysteresis behavior of the input.

CRediT authorship contribution statement

Wei Zhao: Writing – original draft, Software, Methodology, Formal analysis. **Yu-Qun Han:** Writing – review & editing, Methodology, Funding acquisition. **Shan-Liang Zhu:** Writing – review & editing, Software, Methodology, Formal analysis.

Funding

This work was supported by the Shandong Provincial Natural Science Foundation, China (No. ZR2020QF055).

Declaration of competing interest

The authors declare that they have no known competing financial interests or personal relationships that could have appeared to influence the work reported in this paper.

Data availability

Data sharing is not applicable to this article as no datasets were generated or analyzed during the current study.

References

Bikas, L. N., & Rovithakis, G. A. (2019). Combining prescribed tracking performance and controller simplicity for a class of uncertain MIMO nonlinear systems with input quantization. *IEEE Transactions on Automatic Control*, *64*(3), 1228–1235. http://dx.doi.org/10.1109/TAC.2018.2847458.

Capuano, R., Vaiana, N., Pellecchia, D., & Rosati, L. (2022). A solution algorithm for a modified bouc-wen model capable of simulating cyclic softening and pinching phenomena. *IFAC-PapersOnLine*, *55*(20), 319–324. http://dx.doi.org/10.1016/j.ifacol.2022.09.115.

Chen, C. L., Liu, Y. J., & Wen, G. X. (2014). Fuzzy neural network-based adaptive control for a class of uncertain nonlinear stochastic systems. *IEEE Transactions on Cybernetics*, *44*(5), 583–593. http://dx.doi.org/10.1109/TCYB.2013.2262935.

Deng, X. F., Zhang, C., & Ge, Y. (2022). Adaptive neural network dynamic surface control of uncertain strict-feedback nonlinear systems with unknown control direction and unknown actuator fault. *Journal of the Franklin Institute*, *359*(9), 4054–4073. http://dx.doi.org/10.1016/j.jfranklin.2022.04.010.

Du, Y., Zhu, S. L., Zhai, L. L., & Han, Y. Q. (2023). Switching threshold-based event-triggered adaptive asymptotic tracking control for stochastic nonlinear systems with full-state constraints. *International Journal of Robust and Nonlinear Control*, *33*(13), 7908–7928. http://dx.doi.org/10.1002/rnc.6803.

Echreshavi, Z., Farbood, M., & Shasadeghi, M. (2022). Fuzzy event-triggered integral sliding mode control of nonlinear continuous-time systems. *IEEE Transactions on Fuzzy Systems*, *30*(7), 2347–2359. http://dx.doi.org/10.1109/TFUZZ.2021.3081866.

Gao, T. T., Li, T. S., Liu, Y. J., & Tong, S. C. (2022). IBLF-based adaptive neural control of state-constrained uncertain stochastic nonlinear systems. *IEEE Transactions on Neural Networks and Learning Systems*, *33*(12), 7345–7356. http://dx.doi.org/10.1109/TNNLS.2021.3084820.

Han, Y. Q. (2020). Adaptive output-feedback tracking control for a class of nonlinear systems with input saturation: A multi-dimensional Taylor network-based approach. *International Journal of Systems Science*, *51*(13), 2471–2482. http://dx.doi.org/10.1080/00207721.2020.1797226.

Han, Y. Q., He, W. J., Li, N., & Zhu, S. L. (2021). Adaptive tracking control of a class of nonlinear systems with input delay and dynamic uncertainties using multi-dimensional Taylor network. *International Journal of Control, Automation and Systems*, *19*(12), 4078–4089. http://dx.doi.org/10.1007/s12555-020-0708-y.

Han, Y. Q., He, W. J., Li, N., & Zhu, S. L. (2022). Tracking control for large-scale switched nonlinear systems subject to asymmetric input saturation and output hysteresis: A new adaptive network-based approach. *International Journal of Robust and Nonlinear Control*, *32*(14), 8052–8072. http://dx.doi.org/10.1002/rnc.6258.

Han, Y. Q., Li, N., He, W. J., & Zhu, S. L. (2021). Adaptive multi-dimensional Taylor network funnel control of a class of nonlinear systems with asymmetric input saturation. *International Journal of Adaptive Control and Signal Processing*, *35*(5), 713–726. http://dx.doi.org/10.1002/acs.3224.

He, W. J., Han, Y. Q., Li, N., & Zhu, S. L. (2021). Novel adaptive controller design for a class of switched nonlinear systems subject to input delay using multi-dimensional Taylor network. *International Journal of Adaptive Control and Signal Processing*, *36*(3), 607–624. http://dx.doi.org/10.1002/acs.3362.

He, W. J., Zhu, S. L., Li, N., & Han, Y. Q. (2023). Adaptive finite-time control for switched nonlinear systems subject to multiple objective constraints via multi-dimensional Taylor network approach. *ISA Transactions*, *136*, 323–333. http://dx.doi.org/10.1016/j.isatra.2022.10.048.

Jin, X., & Li, Y. X. (2021). Adaptive fuzzy control of uncertain stochastic nonlinear systems with full state constraints. *Information Sciences*, *574*, 625–639. http://dx.doi.org/10.1016/j.ins.2021.07.056.

Lan, J., Liu, Y. J., Liu, L., & Tong, S. C. (2021). Adaptive output feedback tracking control for a class of nonlinear time-varying state constrained systems with fuzzy dead-zone input. *IEEE Transactions on Fuzzy Systems*, *29*(7), 1841–1852. http://dx.doi.org/10.1109/TFUZZ.2020.2986705.

Li, Y. X., Hu, X. Y., Ahn, C. K., Hou, Z. S., & Kang, H. H. (2022). Event-based adaptive neural asymptotic tracking control for networked nonlinear stochastic systems. *IEEE Transactions on Network Science and Engineering*, *9*(4), 2290–2300. http://dx.doi.org/10.1109/TNSE.2022.3161645.

Li, K. W., & Li, Y. M. (2021). Adaptive neural network finite-time dynamic surface control for nonlinear systems. *IEEE Transactions on Neural Networks and Learning Systems*, *32*(12), 5688–5697. http://dx.doi.org/10.1109/TNNLS.2020.3027335.

Li, Y. M., Tong, S. C., & Li, T. S. (2012). Adaptive fuzzy output feedback control of uncertain nonlinear systems with unknown backlash-like hysteresis. *Information Sciences*, *198*, 130–146. http://dx.doi.org/10.1016/j.ins.2012.02.050.

Li, N., Zhu, S. L., He, W. J., & Han, Y. Q. (2022). Controller design for nonlinear systems subject to both input saturation and asymmetry time-varying state constraints: A novel network-based approach. *International Journal of Adaptive Control and Signal Processing*, *36*(12), 3124–3141. http://dx.doi.org/10.1002/acs.3503.

Liang, B. Y., Zheng, S. Q., Ahn, C. K., & Liu, F. (2022). Adaptive fuzzy control for fractional-order interconnected systems with unknown control directions. *IEEE Transactions on Fuzzy Systems*, *30*(1), 75–87. http://dx.doi.org/10.1109/TFUZZ.2020.3031694.

Liu, H., Li, X. H., Liu, X. P., & Wang, H. Q. (2020). Adaptive neural network prescribed performance bounded-H_∞ tracking control for a class of stochastic nonlinear systems. *IEEE Transactions on Neural Networks and Learning Systems*, *31*(6), 2140–2152. http://dx.doi.org/10.1109/TNNLS.2019.2928594.

Liu, Z., Lu, K. X., Lai, G. Y., Chen, C. L. P., & Zhang, Y. (2021). Indirect fuzzy control of nonlinear systems with unknown input and state hysteresis using an alternative adaptive inverse. *IEEE Transactions on Fuzzy Systems*, *29*(3), 500–514. http://dx.doi.org/10.1109/TFUZZ.2019.2952783.

Liu, Z., Yu, J. P., & Lam, H. K. (2023). Passivity-based adaptive fuzzy control for stochastic nonlinear switched systems via T–S fuzzy modeling. *IEEE Transactions on Fuzzy Systems*, *31*(4), 1401–1408. http://dx.doi.org/10.1109/TFUZZ.2022.3195645.

Ma, Z. Y., Kang, H. B., & Ma, H. J. (2022). Adaptive output-feedback asymptotic tracking control for a class of nonlinear systems with actuator failure. *Journal of the Franklin Institute*, *359*(5), 1881–1898. http://dx.doi.org/10.1016/j.jfranklin.2022.01.037.

Meng, Q. T., Ma, Q., & Zhou, G. P. (2022). Adaptive output feedback control for stochastic uncertain nonlinear time-delay systems. *IEEE Transactions on Circuits and Systems II: Express Briefs*, *69*(7), 3289–3293. http://dx.doi.org/10.1109/TCSII.2022.3152523.

Meng, W. C., Yang, Q. M., & Sun, Y. X. (2015). Adaptive neural control of nonlinear MIMO systems with time-varying output constraints. *IEEE Transactions on Neural Networks and Learning Systems*, *26*(5), 1074–1085. http://dx.doi.org/10.1109/TNNLS.2014.2333878.

Pan, H. H., Zhang, D., Sun, W. C., & Yu, X. H. (2022). Event-triggered adaptive asymptotic tracking control of uncertain MIMO nonlinear systems with actuator faults. *IEEE Transactions on Cybernetics*, *52*(9), 8655–8667. http://dx.doi.org/10.1109/TCYB.2021.3061888.

Qi, W. H., Zong, G. D., Hou, Y. K., & Chadli, M. (2023). SMC for discrete-time nonlinear semi-Markovian switching systems with partly unknown semi-Markov kernel. *IEEE Transactions on Automatic Control*, *68*(3), 1855–1861. http://dx.doi.org/10.1109/TAC.2022.3169584.

Qiu, J. B., Sun, K. K., Rudas, I. J., & Gao, H. J. (2020). Command filter-based adaptive NN control for MIMO nonlinear systems with full-state constraints and actuator hysteresis. *IEEE Transactions on Cybernetics*, *50*(7), 2905–2915. http://dx.doi.org/10.1109/TCYB.2019.2944761.

Ruan, Z. W., Yang, Q. M., Sam Ge, S. Z., & Sun, Y. X. (2022). Adaptive fuzzy fault tolerant control of uncertain MIMO nonlinear systems with output constraints and unknown control directions. *IEEE Transactions on Fuzzy Systems*, *30*(5), 1224–1238. http://dx.doi.org/10.1109/TFUZZ.2021.3055336.

Song, Z. B., Li, P., Wang, Z., Huang, X., & Liu, W. H. (2020). Adaptive tracking control for switched uncertain nonlinear systems with input saturation and unmodeled dynamics. *IEEE Transactions on Circuits and Systems II: Express Briefs*, *67*(12), 3152–3156. http://dx.doi.org/10.1109/TCSII.2020.2966298.

Su, X. H., Liu, Z., Zhang, Y., & Chen, C. L. (2021). Event-triggered adaptive fuzzy tracking control for uncertain nonlinear systems preceded by unknown Prandtl–Ishlinskii hysteresis. *IEEE Transactions on Cybernetics*, *51*(6), 2979–2992. http://dx.doi.org/10.1109/TCYB.2019.2949022.

Sui, S., Chen, C. L. P., & Tong, S. C. (2019). Fuzzy adaptive finite-time control design for nontriangular stochastic nonlinear systems. *IEEE Transactions on Fuzzy Systems*, *27*(1), 172–184. http://dx.doi.org/10.1109/TFUZZ.2018.2882167.

Sun, C. B., Wang, S. B., & Yu, H. S. (2023). Finite-time sliding mode control based on unknown system dynamics estimator for nonlinear robotic systems. *IEEE Transactions on Circuits and Systems II: Express Briefs*, *70*(7), 2535–2539. http://dx.doi.org/10.1109/TCSII.2023.3243570.

Sun, W., Xia, J. W., Zhuang, G. M., Huang, X., & Shen, H. (2019). Adaptive fuzzy asymptotically tracking control of full state constrained nonlinear system based on a novel nussbaum-type function. *Journal of the Franklin Institute*, *356*(4), 1810–1827. http://dx.doi.org/10.1016/j.jfranklin.2018.11.023.

Vaiana, N., & Rosati, L. (2023). Analytical and differential reformulations of the vaiana–rosati model for complex rate-independent mechanical hysteresis phenomena. *Mechanical Systems and Signal Processing*, *199*, Article 110448. http://dx.doi.org/10.1016/j.ymssp.2023.110448.

Vaiana, N., & Rosati, L. (2023). Classification and unified phenomenological modeling of complex uniaxial rate-independent hysteretic responses. *Mechanical Systems and Signal Processing*, *182*, Article 109539. http://dx.doi.org/10.1016/j.ymssp.2022.109539.

Wang, F., Liu, Z., Zhang, Y., & Chen, C. L. P. (2016). Adaptive fuzzy control for a class of stochastic pure-feedback nonlinear systems with unknown hysteresis. *IEEE Transactions on Fuzzy Systems*, *24*(1), 140–152. http://dx.doi.org/10.1109/TFUZZ.2015.2446531.

Wang, F. L., & Long, L. J. (2022). Switched-observer-based event-triggered adaptive fuzzy funnel control for switched nonlinear systems. *IEEE Transactions on Fuzzy Systems*, *30*(6), 1773–1787. http://dx.doi.org/10.1109/TFUZZ.2021.3067063.

Wang, H. Q., Shen, L. Y., Wang, D., Niu, B., & Zhao, X. D. (2022). Fast finite-time adaptive neural fault-tolerant tracking control for multi-input multi-output systems with full-state constraints. *International Journal of Adaptive Control and Signal Processing*, *36*(9), 2269–2288. http://dx.doi.org/10.1002/acs.3454.

Wang, L., Sun, W., & Wu, Y. Q. (2022). Adaptive asymptotic tracking control for stochastic nonlinear systems with unknown backlash-like hysteresis. *Journal of Systems Science and Complexity*, *35*(5), 1824–1838. http://dx.doi.org/10.1007/s11424-022-1111-y.

Wu, J., Sun, W., Su, S. F., & Wu, Y. Q. (2023). Adaptive asymptotic tracking control for input-quantized nonlinear systems with multiple unknown control directions. *IEEE Transactions on Cybernetics*, *53*(8), 5216–5225. http://dx.doi.org/10.1109/TCYB.2022.3184492.

Xi, R. P., Zhang, H. G., Liang, Q. K., & Liu, X. (2023). Command filtered adaptive tracking control for a class of random nonlinear systems. *IEEE Transactions on Circuits and Systems II: Express Briefs*, *70*(6), 2087–2091. http://dx.doi.org/10.1109/TCSII.2022.3229346.

Xie, R. M., Guo, C., & Xie, X. J. (2022). Asymptotic tracking control of state-constrained nonlinear systems with time-varying powers. *IEEE Transactions on Cybernetics*, *52*(5), 4073–4078. http://dx.doi.org/10.1109/TCYB.2020.3015273.

Xie, X. J., Wu, Y., & Hou, Z. G. (2022). Further results on adaptive practical tracking for high-order nonlinear systems with full-state constraints. *IEEE Transactions on Cybernetics*, *52*(10), 9978–9985. http://dx.doi.org/10.1109/TCYB.2021.3069865.

Xu, N., Chen, Y., Xue, A. K., Zong, G. D., & Zhao, X. D. (2022). Adaptive tracking control of time-varying delay switched nonstrict-feedback nonlinear systems with unknown backlash-like hysteresis. *International Journal of Adaptive Control and Signal Processing*, *36*(7), 1584–1602. http://dx.doi.org/10.1002/acs.3411.

Zhan, Y. L., Sui, S., & Tong, S. C. (2022). Adaptive fuzzy decentralized dynamic surface control for fractional-order nonlinear large-scale systems. *IEEE Transactions on Fuzzy Systems*, *30*(8), 3373–3383. http://dx.doi.org/10.1109/TFUZZ.2021.3114746.

Zhang, X. Y., Li, B., Li, Z., Yang, C. G., Chen, X. K., & Su, C. Y. (2022). Adaptive neural digital control of hysteretic systems with implicit inverse compensator and its application on magnetostrictive actuator. *IEEE Transactions on Neural Networks and Learning Systems*, *33*(2), 667–680. http://dx.doi.org/10.1109/TNNLS.2020.3028500.

Zhao, W., Han, Y. Q., Zhou, Y. F., & Zhu, S. L. (2024). Adaptive finite-time tracking control of nonlinear systems subject to input hysteresis and multiple objective constraints. *International Journal of Robust and Nonlinear Control*, *34*(15), 10292–10314. http://dx.doi.org/10.1002/rnc.7517.

Zhao, H. P., & Wang, X. T. (2022). Robust $H\infty$ control of switched nonlinear systems under sampled data. *Journal of Systems Science and Complexity*, *35*(5), 1785–1807. http://dx.doi.org/10.1007/s11424-022-1039-2.

Zhao, X. D., Wang, X. Y., Zhang, S., & Zong, G. D. (2019). Adaptive neural backstepping control design for a class of nonsmooth nonlinear systems. *IEEE Transactions on Systems, Man, and Cybernetics: Systems*, *49*(9), 1820–1831. http://dx.doi.org/10.1109/TSMC.2018.2875947.

Zhao, W., Zhu, S. L., Zhou, Y. F., Han, Y. Q., Wang, W. W., & Zhou, Q. H. (2024). Adaptive prescribed performance tracking control for uncertain nonlinear systems with unknown backlash-like hysteresis. *Proceedings of the Institution of Mechanical Engineers. Part I: Journal of Systems and Control Engineering*, *238*(7), 1206–1218. http://dx.doi.org/10.1177/09596518241236978.

Zhu, S. L., & Han, Y. Q. (2022). Adaptive decentralized prescribed performance control for a class of large-scale nonlinear systems subject to nonsymmetric input saturations. *Neural Computing and Applications*, *34*(13), 11123–11140. http://dx.doi.org/10.1007/s00521-022-07032-8.

Zhu, J. Y., Shen, Q. K., & Zhang, T. P. (2023). Neural network-based decentralized adaptive fault-tolerant control for a class of nonlinear interconnected systems with unknown input powers. *International Journal of Adaptive Control and Signal Processing*, *37*(7), 1693–1715. http://dx.doi.org/10.1002/acs.3596.

Zong, G. D., Yang, D., Lam, J., & Song, X. Q. (2022). Fault-tolerant control of switched LPV systems: a bumpless transfer approach. *IEEE/ASME Transactions on Mechatronics*, *27*(3), 1436–1446. http://dx.doi.org/10.1109/TMECH.2021.3096375.